Chapter 3

CHAPTER 3

DFT AND QTAIM STUDIES ON STRUCTURE AND STABILITY OF DOUBLE METAL DOPED GOLD CLUSTERS

In this chapter we have split the works into three sections.

In **section 3.1**, we have used density functional theory (DFT) with B3LYP functional to study the geometrical structures and relative stabilities of neutral and charged double berylium atoms doped gold clusters. The relative stabilities of the clusters are compared on the basis of average binding energies, fragmentation energies and second order difference of energies. The fragmentation energies and second order difference of energies of all the three types of clusters shows the even-odd alternation phenomenon. The nature of bonding interaction is also investigated by using Bader's quantum theory of atoms in molecules (QTAIM). Based on QTAIM results, it is found that Be doped clusters are more stable than the pure Au clusters due to strong covalent interaction between the gold and beryllium metal centres [Bhattacharjee, D., Mishra, B. K., Chakrabartty, A. K. and Deka, R. C. DFT and QTAIM studies on structure and stability of beryllium doped gold clusters. *Computational and Theoretical Chemistry*, 1034:61-72, 2014].

In **section 3.2,** DFT with PW91PW91 functional have been applied to investigate the structures, relative stabilities and electronic properties of small bimetallic neutral, cationic and anionic Au_nMg_2 (n=1-5) clusters. The relative stabilities of the clusters are

compared on the basis of average binding energies, fragmentation energies and second order difference of energies. These parameters show even-odd alternation phenomenon. Vertical ionisation potential, vertical electron affinity values are used to calculate the electronic preoperties. QTAIM is used to explain the nature of bonding interaction. The population analysis is performed to search the transfer of electrons in Mg and Au atoms [Bhattacharjee, D., Mishra, B. K. and Deka, R. C. A DFT study on structure, stabilities and electronic properties of double magnesium doped gold clusters. *RSC Advances*, 4:56571-56581, 2014].

In **section 3.3**, DFT with PW91PW91 functional have been used to analyse the structures, relative stabilities and electronic properties of small bimetallic neutral and charged Au_nAl_2 (n=1-5) clusters. The relative stabilities of the clusters were investigated on the basis of average binding energies, fragmentation energies and second order difference of energies. The electronic preoperties are calculated by using vertical ionisation potential, vertical electron affinity values and these parametrs show even-odd alternation pheneomenon. The nature of bonding interaction is also studied for the first time in Al doped clusters by using QTAIM technique which indicates the presence of covalent bonding in the studied clusters [Bhattacharjee, D., Mishra, B. K. and Deka, R. C. Effect of double aluminium doping on the structure, stability and electronic properties of small gold clusters. *Journal of Materials Science*, 50:4586-4599, 2015].

3.1 DFT STUDIES ON DOUBLE BERYLLIUM DOPED GOLD CLUSTERS

3.1.1 INTRODUCTION

Pure and bimetallic nanoclusters of gold have received considerable attention because of their physical and chemical properties and also due to their wide applications in various scientific fields such as material science, solid state chemistry, catalysis etc[1-6]. In addition to single metal doped clusters, doubly doped clusters are also widely studied in recent days. The group II element beryllium increases hardness and resistance to corrosion when alloyed to certain metals like Al, Co. Cu, Fe and Au etc [7]. For Be-Au clusters, Balducci *et al.* [8] reported the dissociation energy, vibration frequency and bond energy of bimetallic AuBe dimer by using mass spectrometry and DFT. When one or two Be atoms are doped into neutral and cationic gold clusters, these corresponding isomers display an obvious even-odd alternation due to the closed opened-shell effects [9-11]. However, a detail study on neutral and charged clusters together for double Be doped Au clusters are still missing. Therefore, in this present work, we have carried out DFT studies on small doubly Be doped Au clusters to obtain accurate geometric and electronic properties. For the first time, we have performed a systematic study on charged as well as neutral systems together of the above mentioned clusters. The QTAIM method is also implemented for the first time in these clusters which helps to evaluate the topology of the clusters. Our present study can provide powerful platform in the basic understanding of the doubly doped Au clusters and also to the further experimental research. The comparision between charged and neutral Be doped Au clusters are also shown for for the first time in this work.

3.2.2 COMPUTATIONAL DETAILS

All the calculations reported here are performed using GAUSSIAN 09 suits of program package [12]. In the frame work of DFT, the hybrid B3LYP Functional [13,14] are employed to explore the stationary points on the potential energy surface.

Since the relativistic effects play a key role in the structure and energetic of Au-containing clusters, we have used the Los Alamos LANL2DZ [15,16] Effective Core Pseudopotentials (ECP) and valence double-ζ basis sets for Au. For Beryllium atoms, 6–311+G(d) basis set are used. No symmetric constraints are imposed during geometry optimization. The validity of the results obtained at B3LYP level is examined by calculating the Au-Au and Au-Be bond lengths. The calculated Au-Au (2.54 Å) and Au-Be (2.07 Å) bond lengths are in good agreement with the experimental values of 2.49Å [17] and 2.06Å [18], respectively. The relative stabilities of the clusters, are calculated with the help of averaged binding energies Eb(n), fragmentation energies ΔE(n) and second-order difference of energies Δ^2E(n). These three parameters already proved to be a powerful tool to reflect the relative stability of the clusters

For Au_n clusters averaged binding energies $E_b(n)$, fragmentation energies ΔE(n) and second-order difference of energies Δ^2E(n) are calculated using the following formulae:

$$E_b(Au_{n+2}) = [(n+2)E(Au) - E(Au_{n+2})]/(n+2) \quad (3.1.1)$$

$$E_b(Au_{n+2})^q = [E(Au)^q + nE(Au) - E(Au_{n+2})^q]/(n+2) \quad (3.1.2)$$

$$\Delta E\,(Au_{n+2})^q = [E(Au_{n+1})^q + E(Au) - E(Au_{n+2})^q] \quad (3.1.3)$$

$$\Delta^2 E(Au_{n+2})^q = [E(Au_{n+1})^q + E(Au_{n+3})^q - 2E(Au_{n+2})^q] \quad (3.1.4)$$

Where, E(Au) represents the ground state energy of the Au, q is the charge on the cluster, q=0,+1 and -1 for neutral, cationic and anionic clusters, respectively and n is the number of gold atoms associated with the clusters.

Similarly for Au_nBe_2 clusters averaged binding energies $E_b(n)$, fragmentation energies ΔE(n) and second-order difference of energies Δ^2E(n) are calculated using the following formulae:

$$E_b(Au_nM_2)^q = [2E(M)^q + nE(Au) - E(Au_nM_2)^q]/(n+2) \quad (3.1.5)$$

$$\Delta E(Au_nM_2)^q = [E(Au_{n-1}M_2) + E(Au) - E(Au_nM_2)^q] \quad (3.1.6)$$

$$\Delta^2 E\,(Au_nM_2)^q = [E(Au_{n-1}M_2) + E(Au_{n+1}M_2) - 2E(Au_nM_2)^q] \quad (3.1.7)$$

Where, M denotes the Be atom. $E(M_2Au_n)$, E(Au), E(M) denote the total energy of the Be_2Au_n, Au and Be, respectively.

The nature of bonding in the studied clusters is analyzed by using Bader's quantum theory of atoms in molecules (QTAIM) [19-21]. For QTAIM analysis, we have used Gaussian 09 to generate the wave function using the same level of theory from the optimized structures and then used the AIMALL package [22].

3.2.3 RESULTS AND DISCUSSION

3.2.3.1 Structural Study of Au_nBe_2 clusters

To study the effect of doping of Be atoms in Au clusters, first we have optimized a number of Au_nBe_2 cationic, anionic and neutral clusters. The structures obtained in present work for neutral Au clusters are identcal to the previous study[23]. The structures of the clusters are shown in Figure 3.1.1-3.1.3. Putting the Be atoms in different positions we obtained different isomers for a particular cluster and considered only the low energy i.e., the most stable clusters. The most stable clusters are obtained by comparing their relative energies. For $AuBe_2$ we obtained two isomers between which the isomers indicated by A2 in Figures 3.1.1-3.1.3 are found to be most stable. In case of neutral cluster, we obtained only linear isomers whereas in case of charged ones, a triangular structure is also obtained. The shortest Au-Be bond lengths for the most stable clusters are found to be 2.09, 2.03 and 2.19 Å whereas Be-Be bond is found to be 2.13, 2.17 and 2.40 Å for neutral, cationic and anionic clusters, respectively. These bond lengths are in close agreement with the previous theoretical values of 2.06 Å and 2.15 Å for Au-Be and Be-Be bond lengths, respectively [24]. In case of Au_2Be_2 clusters, we studied two different isomers and the most stable structures are indicated by B2 in Figures 3.1.1-3.1.3. Here also we observed a linear isomer for neutral cluster but for charged clusters only strain structures are observed. The calculated shortest Au-Be bond lengths are 2.09, 2.17 and 2.19 Å for neutral, cationic and anionic clusters, respectively. The Be-Be bond length is 2.07 Å which is very close to the previous study [24].

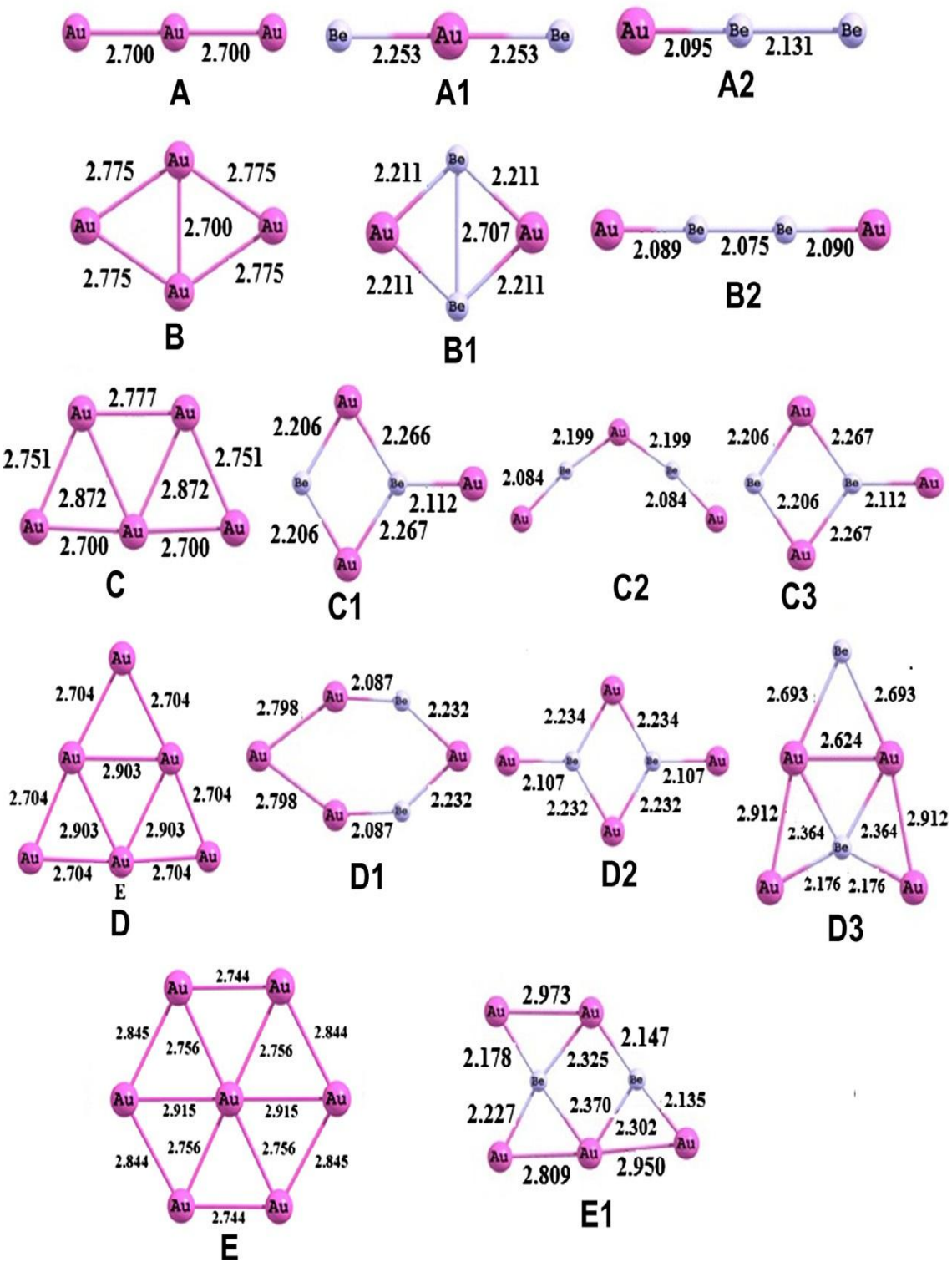

Figure 3.1.1 Structures of neutral Au_{n+2} and Au_nBe_2(n=1-5) clusters.

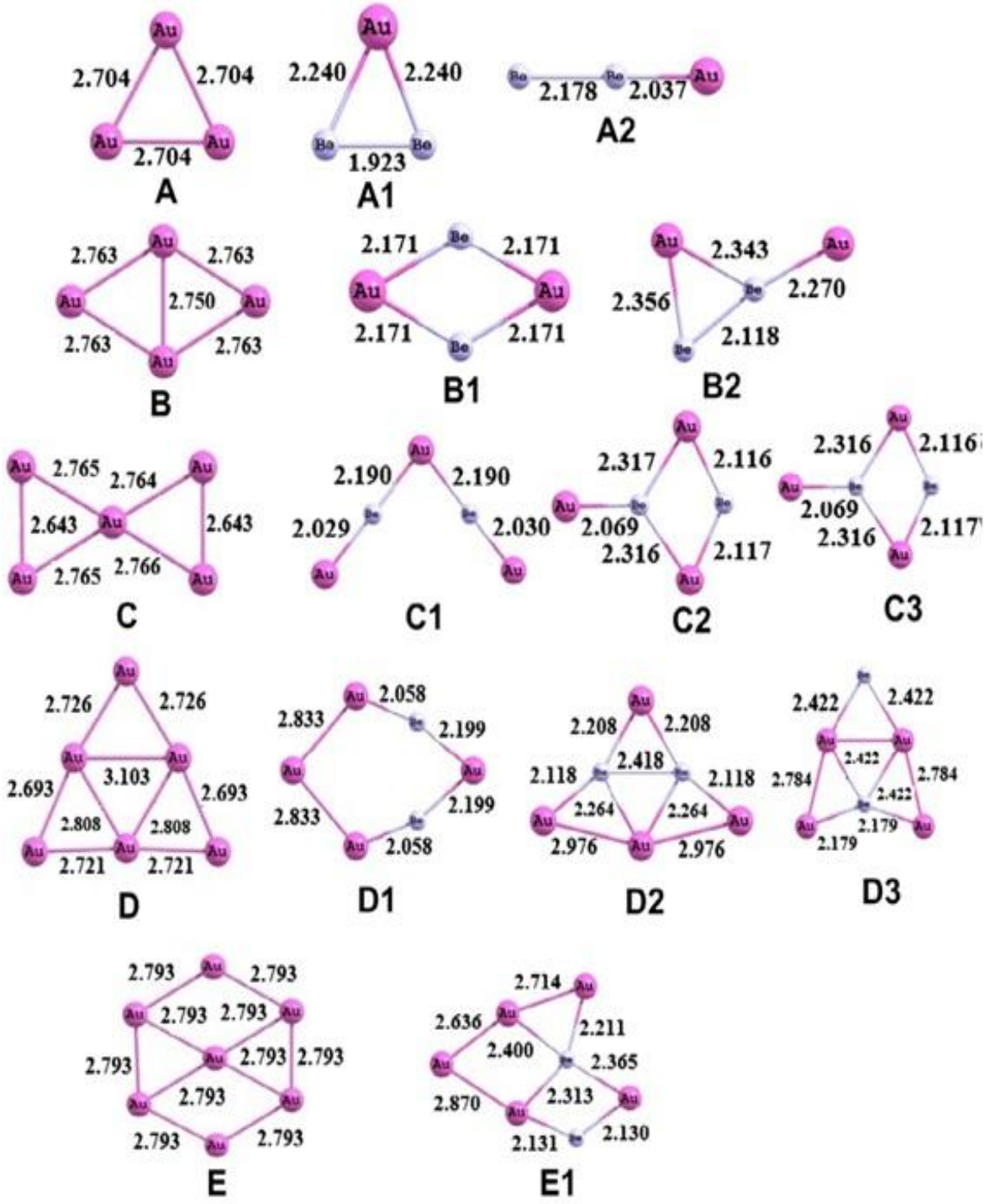

Figure 3.1.2 Structures of cationic Au_{n+2} and Au_nBe_2(n=1-5) clusters.

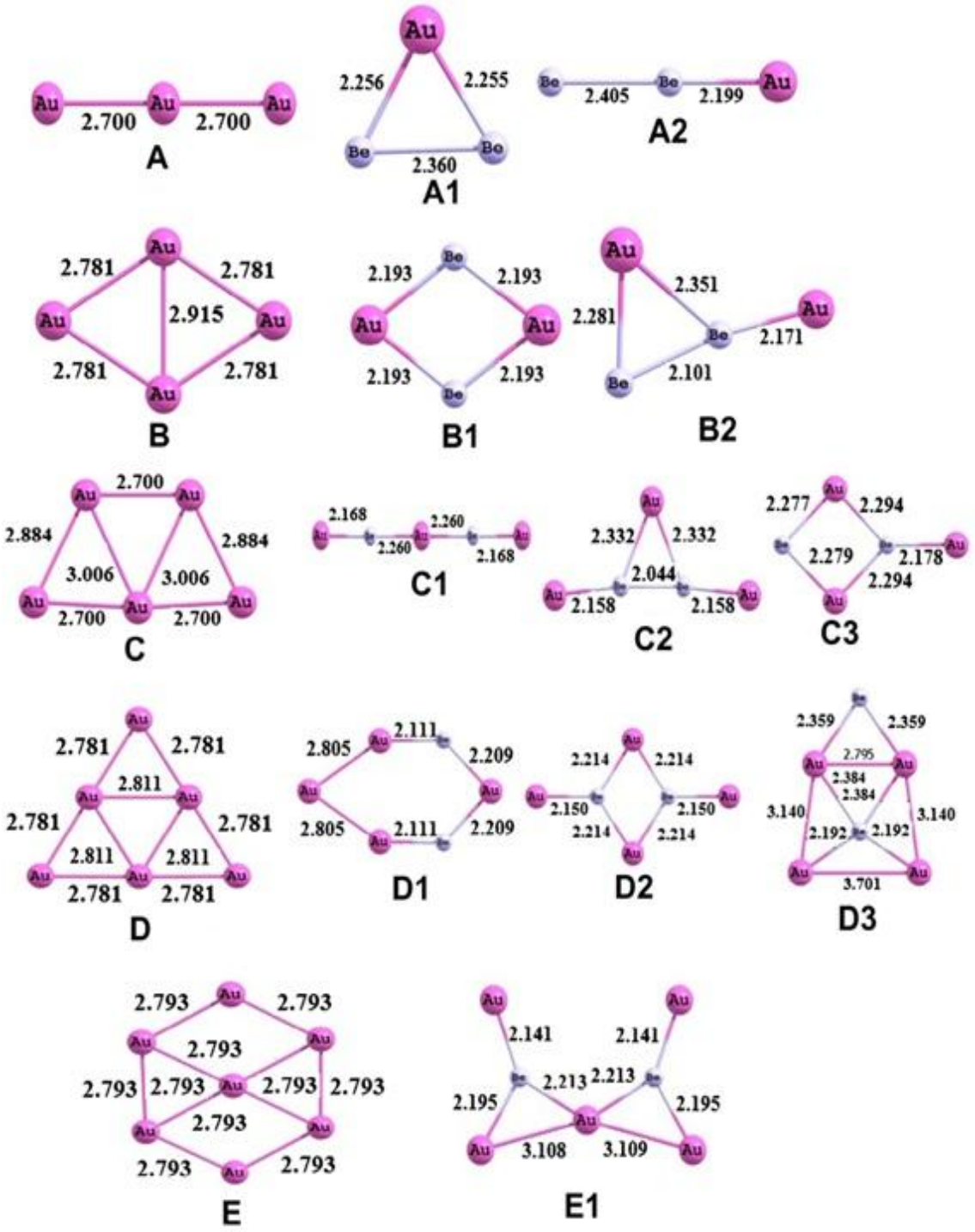

Figure 3.1.3 Structures of anionic Au_{n+2} and Au_nBe_2(n=1-5) clusters.

For Au_3Be_2 clusters, we obtained three different isomers. Here we obtained a linear isomer for the anionic cluster whereas only bent isomers are found for cationic and neutral clusters. The most stable isomers are C3 for neutral and cationic and whereas C1 for anionic clusters. The shortest Au-Be bond lengths are found to be 2.20, 2.06 and 2.16 Å for neutral, cationic and anionic clusters, respectively. In Au_4Be_2 clusters, three different isomers are obtained. The most stable isomers are D2 as shown in Figures 3.1.1-3.1.3. In this case, neutral and charged clusters are found to be of similar structure. The shortest Au-Be bond lengths are calculated as 2.10, 2.20 and 2.15 Å for neutral, cationic and anionic clusters respectively.

Lastly for Au_5Be_2 cluster, we obtained a W-like structure for anionic cluster whereas structures of cationic and neutral clusters are almost similar. The shortest Au-Be bond lengths here are found to be 2.17, 2.21 and 2.19 Å for neutral, cationic and anionic clusters, respectively. Almost all the structures of Au_nBe_2 clusters are found to be plannar.

3.1.3.2 Stability of Au_nBe_2 clusters

The stability of the Au_nBe_2 clusters are calculated in terms of averaged binding energies $E_b(n)$, fragmentation energies $\Delta E(n)$ and second-order difference of energies $\Delta^2E(n)$ using formulas (3.1.1-3.1.7) and plotting them as a function of cluster size (Figures 3.1.4-3.1.6). The binding energy plots clearly indicate that in all the neutral, cationic and anionic clusters, the doping of double Be atoms increases the stability of the gold clusters compared to that of bare clusters. The plot of fragmentation energies $\Delta E(n)$ and second-order difference of energies $\Delta^2E(n)$ for the Au_nBe_2 clusters shows an even-odd alternation. The Au_nBe_2 clusters with odd number of gold atoms are more stable compared to the neighbouring even ones. The stability of charged and neutral clusters on the basis of their binding energies are compared as shown in Figure 3.1.7. This plot indicates that for doubly Be doped Au clusters, the stability varies as neutral < anionic < cationic. Therefore, charge plays a key role in the stability of these clusters.

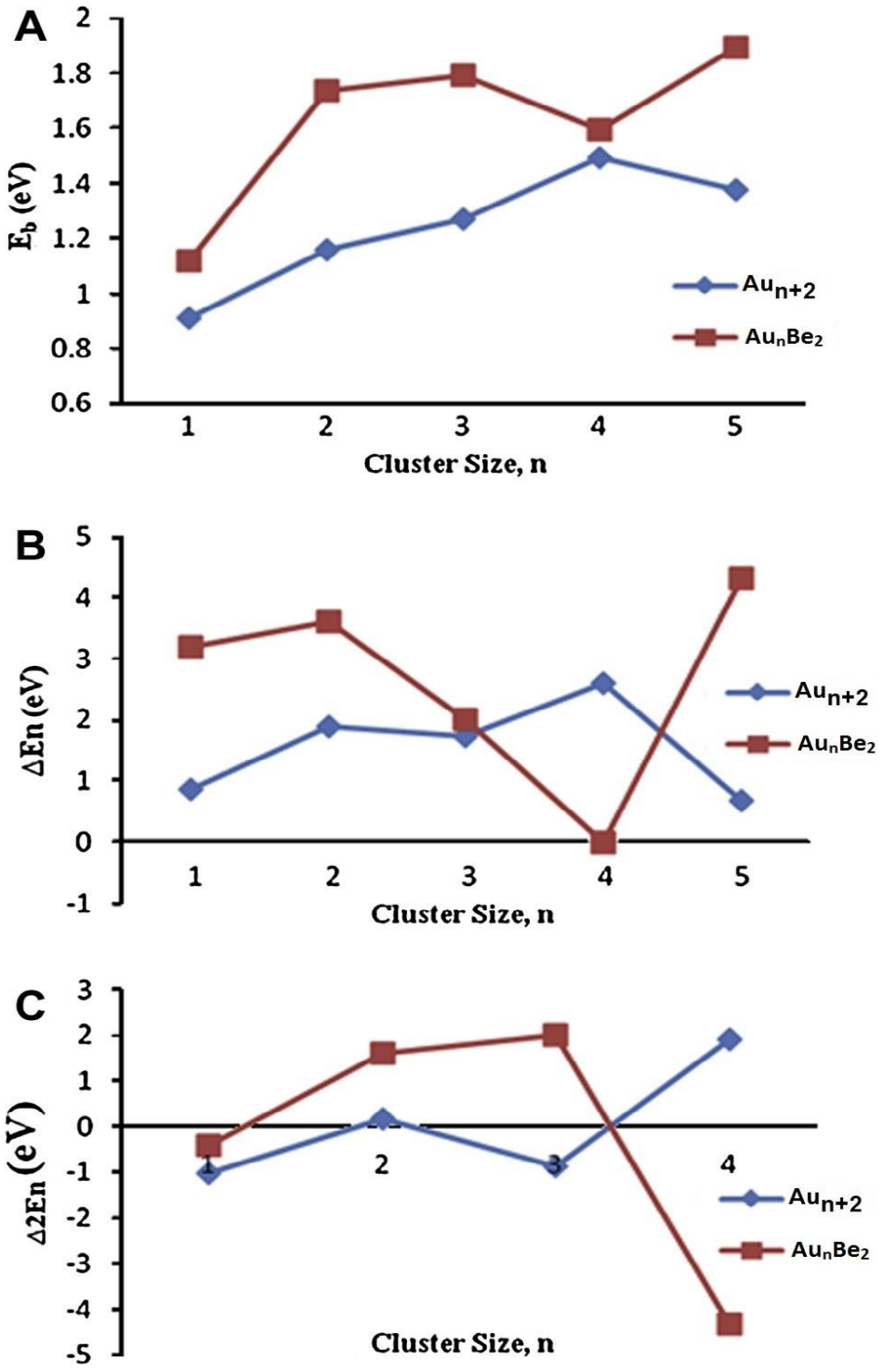

Figure 3.1.4 Size dependence of the **(A)** averaged binding energies Eb(n), **(B)** fragmentation energies ΔE(n) and **(C)** second-order difference of energies Δ_2E(n) and for the lowest energy structures of neutral Au_{n+2} and Au_nBe_2 (n=1–5) clusters.

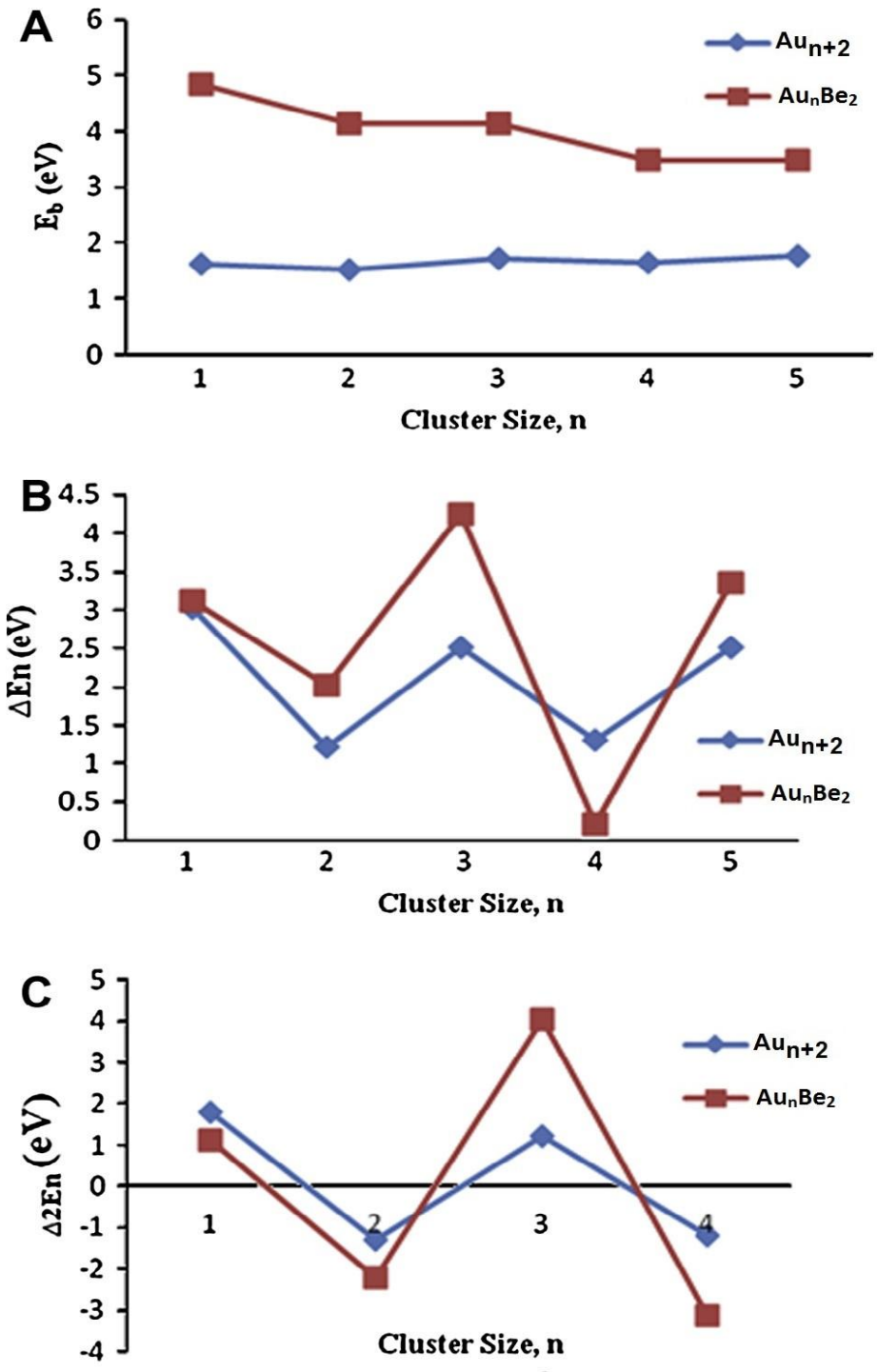

Figure 3.1.5 Size dependence of the **(A)** averaged binding energies Eb(n), **(B)** fragmentation energies ΔE(n) and **(C)** second-order difference of energies Δ_2E(n) and for the lowest energy structures of cationic Au_{n+2} and Au_nBe_2 (n=1–5) clusters.

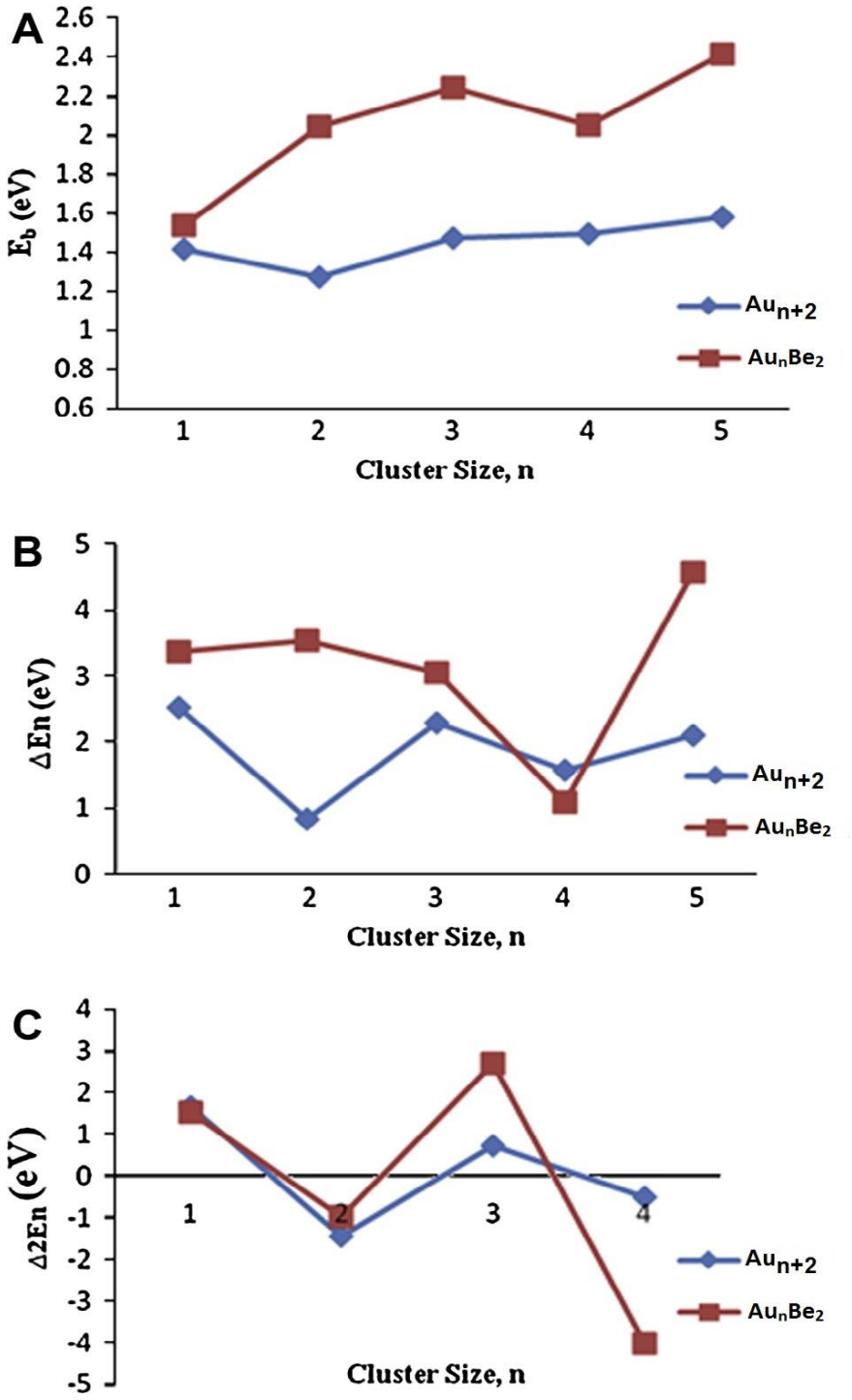

Figure 3.1.6 Size dependence of the **(A)** averaged binding energies Eb(n), **(B)** fragmentation energies ΔE(n) and **(C)** second-order difference of energies Δ_2E(n) and for the lowest energy structures of anionic Au_{n+2} and Au_nBe_2 (n=1–5) clusters.

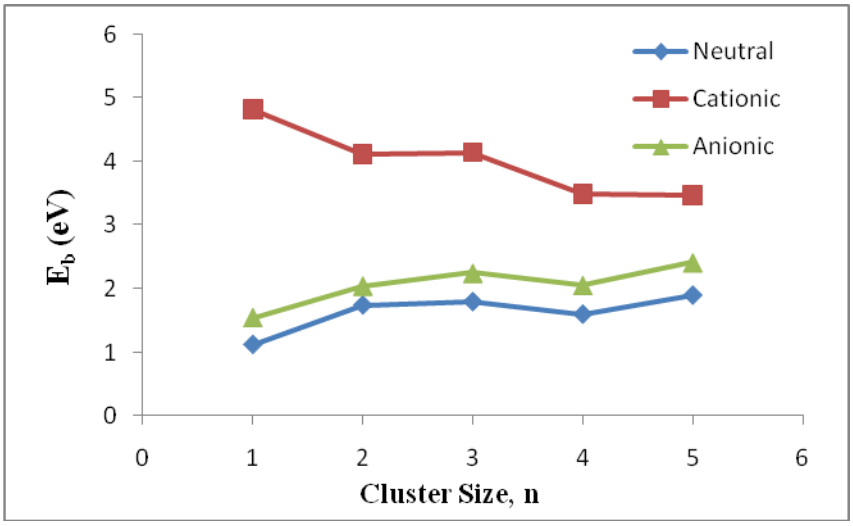

Figure 3.1.7 Comparision of stability of neutral and charged Au_nBe_2 clusters

3.1.3.3 QTAIM analysis

The topology of electron density are calculatd using Bader's quantum theory of atoms in molecules (QTAIM) [19]. The parameters that are used here are the electron density, ρ and the Laplacian of electron density, $\nabla^2\rho$ at the bond critical point (BCP), are local electronic energy density function, H(r) (H(r) is the sum of local kinetic G(r) and potential V(r) energy densities, i.e., H(r) = G(r) + V(r)) and relative kinetic energy density, G(r)/ρ.

In all the Au_nBe_2 clusters, BCPs are present which indicates the interaction between the Au and Be atoms. However, in QTAIM analysis, we cannot take into account all the structures. Our aim is to notice the variation of Be doping in Au clusters. The calcualted values of different parameters that we observed during QTAIM are given in Table 3.1.1 for some selected clusters while the values of some other clusters are provided in Table A.1 of appendix A. The small and positive values obtained for ρ and $\nabla^2\rho$ for the analysed structures in Table 3.1.1 indicates the covalent interaction between Au-Au and Au-Be atoms. However, compared to that of Au-Au bond, bond critical point shifts towards Mg atom in Au-Mg bond as shown in Figure 3.1.8. The negative values of energy density H(r) and value of G(r)/ρ <1 also points

towards the covalent interactions although the degree may not be too high. A small change in the values of H(r) in Au-Au and Au-Be are (H(r) values -0.019 and -0.032 for Au-Au and Au-Be bond) indicates that the covalent character is comparatively higher in Au-Be bond compared to that in Au-Au bond. This may be responsible for increase stability of Be doped gold clusters.

Table 3.1.1 Calculated values of selected bond properties of Au-Au and Au-Be bonds of different Au_nBe_2 clusters.

Cluster	Interaction	ρ	$\nabla^2 \rho$	H(r)	G(r)/ρ
Neutral					
Au_3	Au1 - Au2	0.059	0.135	-0.019	0.896
	Au1 - Au3	0.059	0.135	-0.019	0.896
Au-Be_2	Au-Be	0.068	0.103	-0.032	0.839
	Be-Be	0.061	-0.1	-0.031	0.098
Cationic					
Au_4	Au2 - Au4	0.051	0.112	-0.014	0.842
	Au1 - Au2	0.051	0.112	-0.014	0.832
	Au2 - Au3	0.051	0.112	-0.014	0.832
	Au1 - Au4	0.051	0.112	-0.014	0.832
	Au3 - Au4	0.051	0.112	-0.014	0.832
Au_2-Be_2	Au1 - Be3	0.061	0.097	-0.026	0.82
	Au2 - Be3	0.061	0.097	-0.026	0.82
	Au1 - Be4	0.061	0.097	-0.026	0.82
	Au2 - Be4	0.061	0.097	-0.026	0.82

Continued….

Cluster	Interaction	ρ	$\nabla^2 \rho$	H(r)	G(r)/ρ
Anionic					
Au_4	Au2 - Au4	0.037	0.091	-0.007	0.819
	Au1 - Au2	0.047	0.109	-0.013	0.849
	Au2 - Au3	0.047	0.109	-0.013	0.849
	Au1 - Au4	0.047	0.109	-0.013	0.849
	Au3 - Au4	0.047	0.109	-0.013	0.849
Au_2-Be_2	Au1 - Be3	0.05	0.126	-0.017	0.955
	Au2 - Be3	0.05	0.126	-0.017	0.955
	Au1 - Be4	0.05	0.126	-0.017	0.955
	Au2 - Be4	0.05	0.126	-0.017	0.955

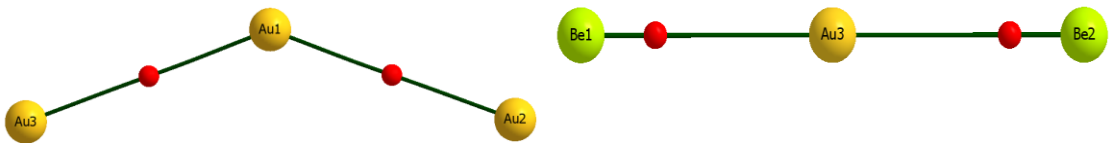

Figure 3.1.8 Shifting of BCP in Au-Au and Au-Be bonds. The red dots indicate BCP.

The further confirmation of covalent interaction have been confirmed by much smaller values of G(r)/ρ than 1 in all the interactions of the clusters as shown in the above table. On observing the basin paths for the different clusters, it clearly confirms that interaction between the Au-Au and Au-Be atoms are significant. Also the presence of ring critical points (RCP) in several clusters confirms the cyclic structures that we obtained during optimisation. For example, we obtained a triangular structure for cationic Au_3, neutral Au4Be2 clusters. The QTAIM analysis confirms this structure by resulting the RCPs as shown in Figure 3.1.9.

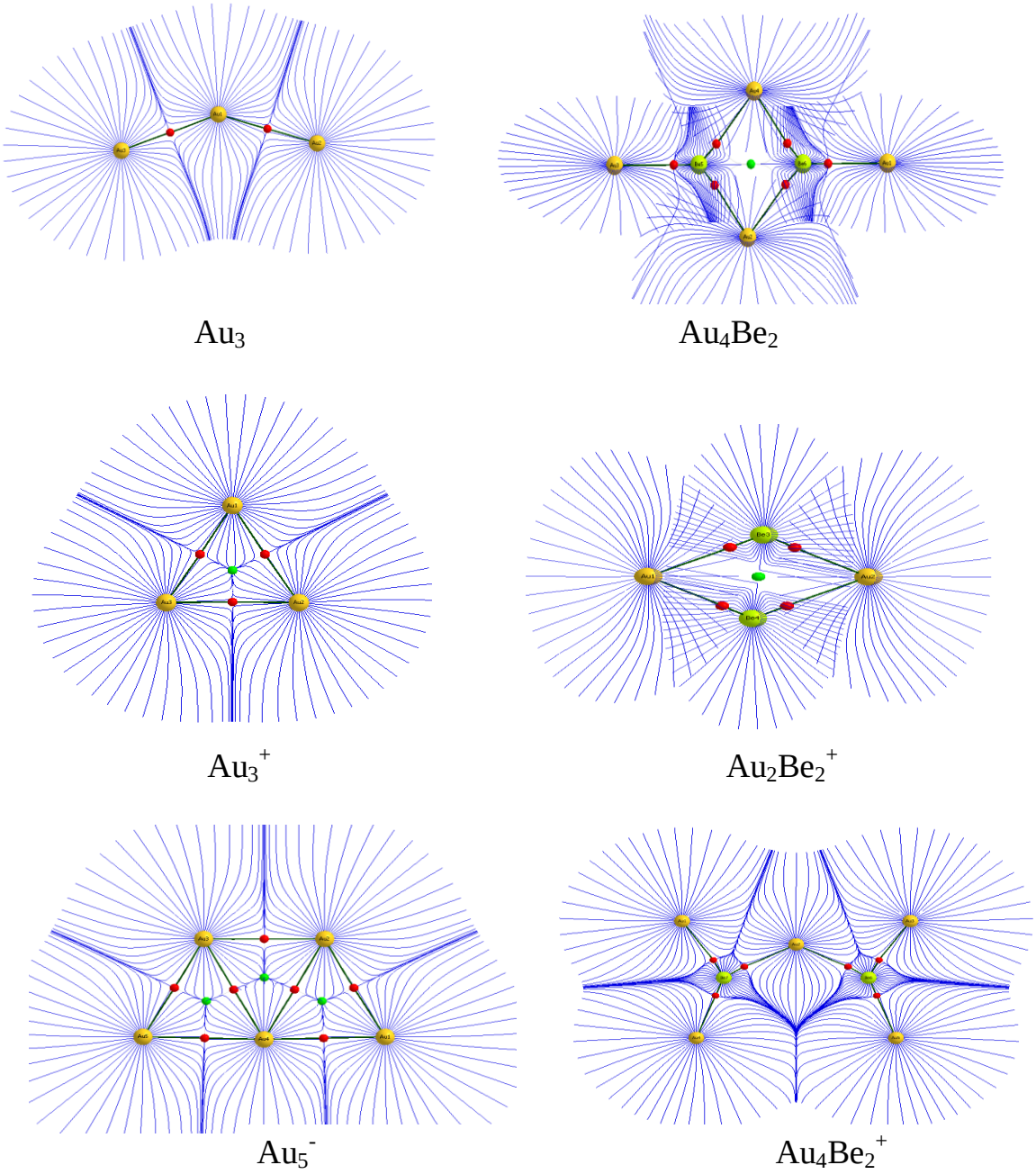

Figure 3.1.9 Trajectory field in some of the Au_n and Au_nBe_2 clusters. Gold and magnesium atoms are represented by yellow and green spheres respectively. Bond paths and basin paths are indicated by dark green and blue lines, while the interatomic surfaces are indicated by dark blue lines. Red and green dots indicate bond critical points and ring critical points, respectively.

3.1.3.4 Natural Charge analysis

Using the same level of theory, we have analysed the variation of charge for doping Be atoms in Au clusters with the help of Mulliken atomic charge localization. The charge analysis reveals that in neutral $AuBe_2$ cluster, the Be atoms have positive charges (0.605) whereas Au has negative charges (-1.211). Similarly, for the cationic $AuBe_2$ cluster, Be atoms possess positive charges (0.847) and Au atoms has negative charge (-0.694). In case of anionic $AuBe_2$ clusters, the charges are 0.178 and -1.357 for Be and Au atoms, respectively. Hence charges transfer may occur from Be atom to Au atom which may be the reason for extra stability of doped clusters. The HOMO-LUMO isosurfaces are also generated for Au_3 and $AuBe_2$ as shown in Figure 3.1.10. The isosurfaces clearly indicate the formation of covalent bonds in both the cases it support the existance of covalent character in accordance with the QTAIM study.

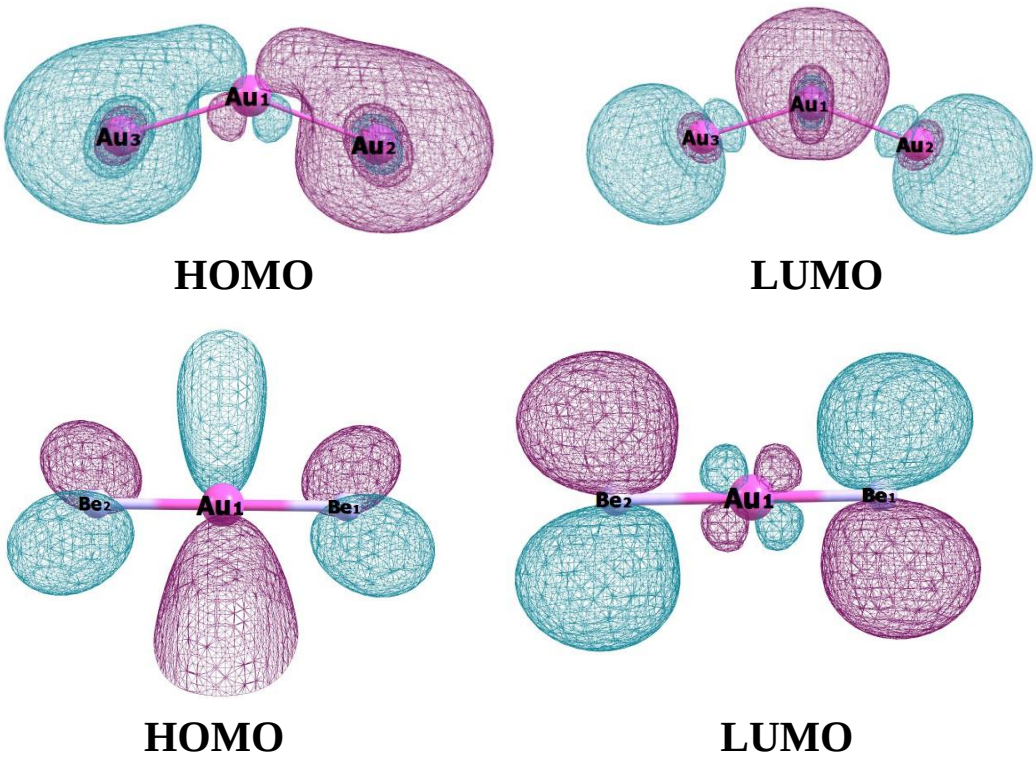

Figure 3.2.10 HOMO and LUMO isosurfaces of Au_3 and $AuBe_2$ clusters

3.1.4 SALIENT OBSERVATIONS

We have presented a systematic study on structural and stability of double Be atoms doped Au_n (n=1-7) clusters by DFT using B3LYP functional. The mainly reveals the following points:

1. The stability of Au clusters can be enhanced by Be atoms. Charge plays a major role in the strcture of the clusters. Almost all the Au_nBe_2 clusters adopt plannar structures.
2. The stability study shows an even-odd alternation and the odd Au numbered clusters are found to be more stable. The stability trends here indicates the greater stability of cationic clusters.
3. QTAIM analysis reveals that the values of electron density, ρ, and its Laplacian, $\nabla^2\rho$ at the Au-Au and Au-Be BCPs are very small and positive. The other two parameters viz local electronic densities, H(r), are all negative and relative kinetic energy density $G(r)/\rho$ has values less than one. All these parameters confirm the presence of covalent interactions in the studied clusters.
4. The natural charge analysis confirms the transfer of charge from Be to Au atoms.

3.2 DFT STUDY ON DOUBLE MAGNESIUM DOPED GOLD CLUSTERS

4.2.1 INTRODUCTION

The alkaline earth element magnesium (Mg) is extremely reactive in the free state. It is resistance to corrosion when alloyed to certain metals like Fe, Ni, Cu, Co etc.[25]. For Mg doped Au clusters, Kyasu *et al.*[26] performed anion photoelectronic study on Au_nMg^- (n=2-7) clusters. Majumdar *et al.* [27] theoretically observed the structure and bonding of Au_5Mg cluster. They found that Au_5Mg cluster adopt planar structure simillar to Au_6. Li *et al.* [28] systematically analysed the properties of anionic Au_nMg(n=1-8) clusters and found that lowest energy structures for Au_nMg clusters are different to that of the bare Au clusters. However, to the best of our knowledge, no systematic theoretical investigations into Mg_2Au_n clusters have been performed. It is interestiong and promising to see that if two Mg atoms are doped in gold clusters together, do their structures and properties differ from those of bare gold clusters? Therefore, by applying DFT we have studied the structural and electronic properties of Au clusters doped with two Mg atoms, Au_nMg_2 (n=1-5).

During this study, we have optimised a certain type of structures by doping Mg atoms at different positions in the bare Au clusters. The importance of this work lies in the fact that nanosized Au clusters already shows tremendous catalytic activity for different types of reactions and doping of a metal can further enhanced its catalytic property. The novelity of the work with reference to the previous works lies in the facts that for the first time we have studied the all neutral and charged clusters for two Mg metal doped Au clusters and compared with the pure ones. Also for the first time, we have performed QTAIM study in the Al doped Au clusters to study the bond parameters. Our present study can provide powerful guidedlines to consider the Mg doped Au clusters in the further experimental research.

3.2.2 COMPUTATIONAL DETAILS

To generate the initial structures of the neutral state, we have used a classical annealing simulation using the Forcite Plus code as encoded in the MATERIAL STUDIO software [29]. The Universal force field (UFF) [30] is adopted to perform

this simulation which already provides reliable results for gold based systems [31,32]. The cut-off radius is chosen to be 15.5 Å and NVE ensemble has been used. A total of 100 annealing cycles are simulated with a temperature range of 200 K to 1000 K. The most stable structures obtained by this simulation used as input for DFT studies. In the DFT study, we have used the gradient-corrected exchange and correlation functional of Perdew-Wang (PW91PW91) [33] to explore the stationary points on the potential energy surface. PW91PW91 functional is proved to be succesful in the previous study of Mg doped Au clusters [27,28]. To consider the relativistic effects Au, the Los Alamos LANL2DZ Effective Core Pseudopotentials (ECP) and valence double-ζ basis sets are used for Au [15,16]. The Mg atoms are treated with 6–311+G(d) basis set. No any symmetry constraints are imposed during optimization of neutral and charged clusters. In order to obtain the lowest energy doped isomers, initial structures are constructed substituting Au atoms by Mg atoms in the pure gold structures at various attaching sites. The most stable clusters are obtained by comparying their relative energies. For all the structures, the vibrational frequencies are found to be positive confirming them to be at energy minima. The zero-point vibrational energy corrections have also considered in all the calculations. The stability of the clusters are described with the help of binding energy, relative stability, ionization potential, electron detachment energy as well as chemical hardness as a function of clusters size. All the calculations are performed using the GAUSSIAN 09 suits of program [12]. The nature of bonding in the clusters are studied by QTAIM method with the help of AIMALL package [22]..

3.2.3 RESULTS AND DISCUSSION

3.2.3.1 Structural study of Au_nMg_2 clusters

The optimized geometries of various neutral and charged Au_n and Au_nMg_2 clusters are presented in Figure 3.2.1 to 3.2.3. Among different isomers obtained for a particular cluster, the energy of the most stable isomer is taken as zero and energy of the others are compared relative to it.

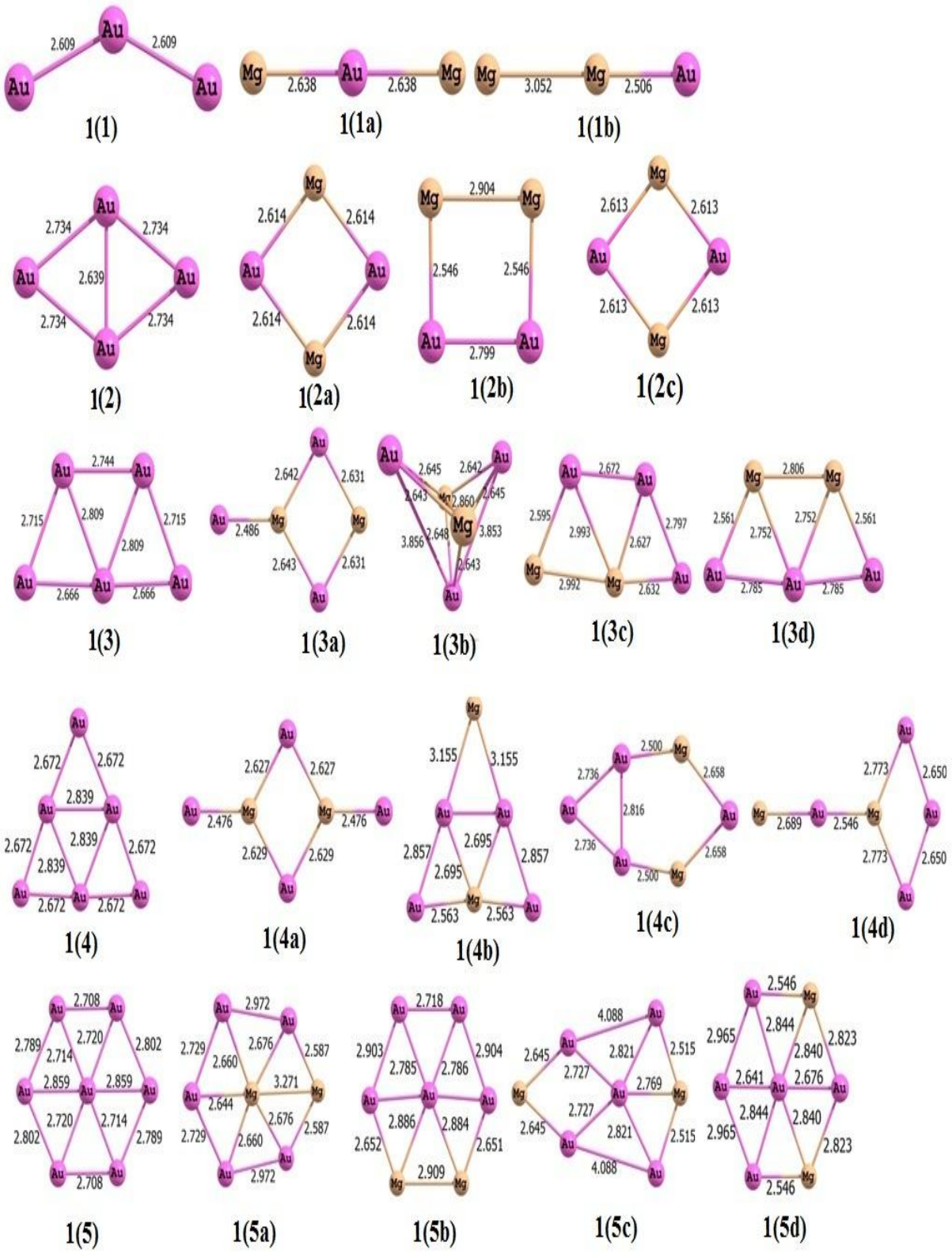

Figure 3.2.1 Optimized structures of neutral Au_{n+2} and Au_nMg_2 (n = 1–5) clusters

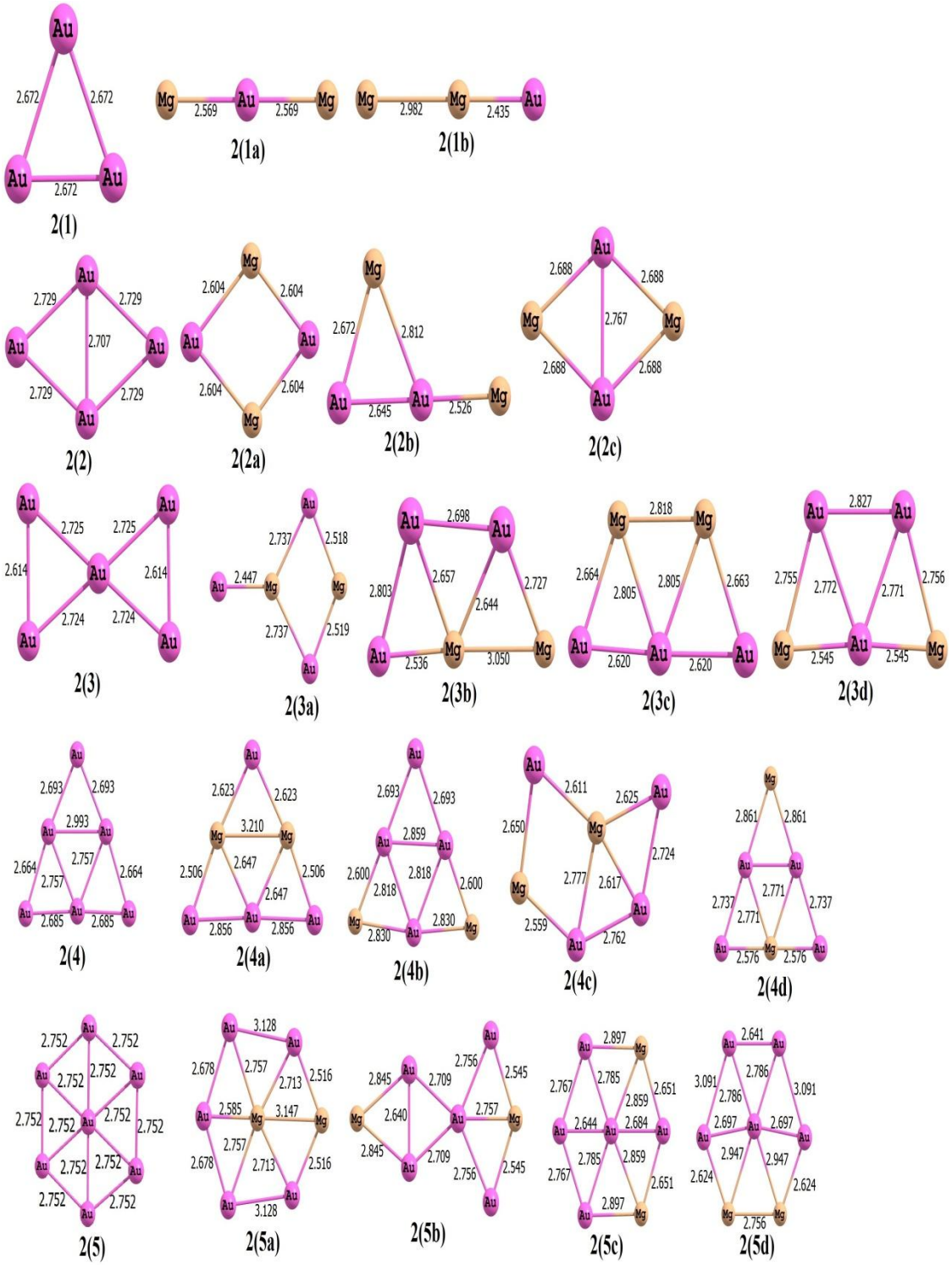

Figure 3.2.2 Optimized structures of cationic Au_{n+2} and Au_nMg_2 (n = 1–5) clusters.

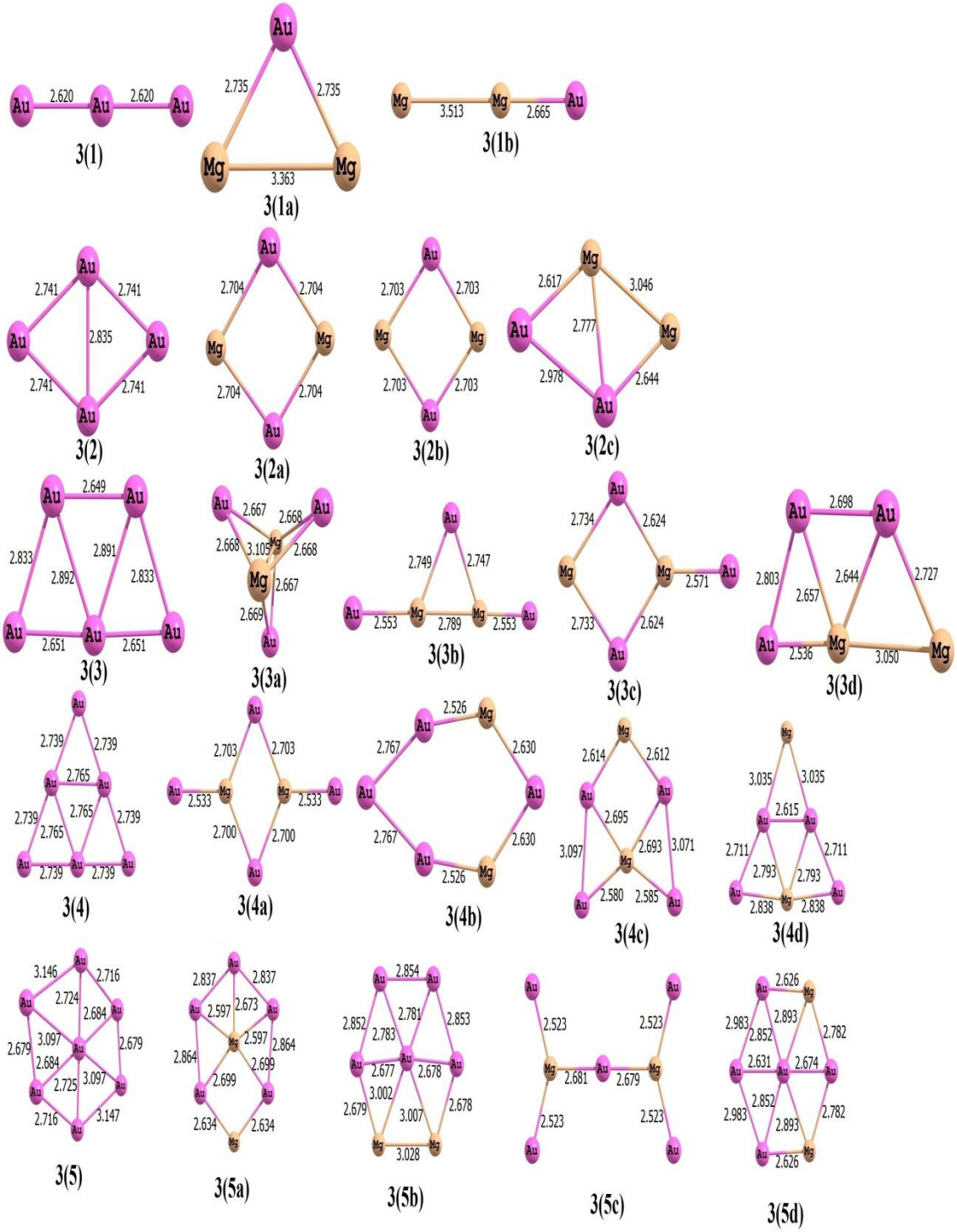

Figure 3.2.3 Optimized structures of anionic Au_{n+2} and Au_nMg_2 (n = 1–5) clusters.

3.2.3.1.1 Neutral clusters

The neutral Au clusters are taken as identcal to the previous study [23]. From Figure 3.2.1, it can be be seen that in doped clusters, the most stable structure for $AuMg_2$ is 1(1a) having a linear shape. The Au-Mg bond lengths are found to be 2.638 Å. The other isomer, 1(1b) is found to be higher in enrgy compared to 1(1a) by 0.22eV. The structure 1(2a) with square planar shape is found to be most stable for Au_2Mg_2 having symmetry D_{2h}. The Au-Mg bonds are founds to be 2.614 Å. In case of Au_3Mg_2 clusters, the most stable structure is 1(3a) with symmetry C1. Here we also obtained a 3D isomer-1(3b) which is higher in energy than 1(3a) by 0.01 eV. Thus a transition from 2D to 3D is obtained at Au_3Mg_2 for the neutral clusters. For Au_4Mg_2, the most stable isomer is 1(4a). It has symmetry C_{2V} and have shortest Au-Mg distance of 2.476 Å. This bond length is in good agreement with that of 2.56 Å for the single Mg doped cluster [27]. At last, a planar isomer 1(5a) having symmetry C_{2V} is found as the most stable structure for Au_5Mg_2. The calculated values of shortest Au-Mg and Au-Au bond lengths are 2.587 and 2.729 Å, respectively. Therofore, for neutral clusters we obeserved 2D structures except 1(3b) for which 3D structure is observed.

3.2.3.1.1 Charged Clusters

The charged (cationic and anionic) isomers for Au_{n+2} and Au_nMg_2 (n = 1–5) are shown in Figures 3.2.2 and 3.2.3. For $AuMg_2^+$, the most stable cluster is 2(1a) having the linear shape. The stable isomers are found to be 2(2a), 2(3a), 2(4a) and 2(5a) for $Au_2Mg_2^+$, $Au_3Mg_2^+$, $Au_4Mg_2^+$ and $Au_5Mg_2^+$, respectively as shown in Figure 3.2.2. For cationic clusters, we obtained only 2D planar structures and no any transition to 3D structure seems to occur. On comparing the doped structures with that of the bare ones, it shows that apart from $AuMg_2$ and Au_3Mg_2, the stable isomers for other clusters are found to be simillar to the bare clusters. However, high energy isomers such as 2(2b), 2(4c) and 2(5b) along with stable isomers of $AuMg_2$ and Au_3Mg_2 adopt different geometries to that of the pure gold counterpart. For anionic clusters, the most stable isomers are found to be 3(1a), 3(2a), 3(3a), 3(4a) and 3(5a) for $AuMg_2^-$, $Au_2Mg_2^-$, $Au_3Mg_2^-$, $Au_4Mg_2^-$ and $Au_5Mg_2^-$, respectively as shown in Figure 3.2.3. In this study, a

transition from 2D to 3D cluster occurs at $Au_3Mg_2^-$. Also the isomers 3(3b), 3(3c), 3(4a), 3(4b), 3(4c) and 3(5c) have different geometries to those of pure gold clusters. These results indicate that doubly doped Mg atoms can play a key role to effect the geometries of the ground-state charged Au_n clusters also.

3.2.3.2 Stability of Au_nMg_2 clusters

The relative stabilities of the Au_nMg_2 clusters are calculated in terms of averaged binding energies per atom, (E_b) fragmentation energies, $\Delta E(n)$, and second-order difference of energies, $\Delta^2 E$, using formulae (3.1.1-3.1.7) given in the previus section 3.1 (where M=Mg).

3.2.3.2.1 Binding energies per atom

The variation of binding energies per atom (E_b) for the most stable isomers as a function of cluster size is shown in Figure 3.2.4. The binding energy per atom for the pure cluster increases with cluster size for the neutral clusters as shown in the figure. Therefore, the clusters continue to gain energy during the growth process. However, for the charged clusters, the B.E. values show an even-odd alternation. For neutral and anionic doped clusters, we obtained a sharp peak at n=4 and n=3, 5 respectively, which indicates that of these clusters posses higher stability in the region n=1-5. However, for the cationic doped clusters, the E_b values decrease with cluster size. The binding energy plots (Figure 3.2.4) suggested that in all the neutral, cationic and anionic clusters, the doping of two Mg atoms increase the stability of the Au clusters. In the anionic clusters, the variation of the binding energy plot is found to be similar to that of the previous study of on singly doped clusters by Li *et al.* [28]. The comparison of binding energies of charged and neutral clusters (Figure 3.2.5), reveals the order of stability as: neutral < anionic < cationic for Mg doped clusters.

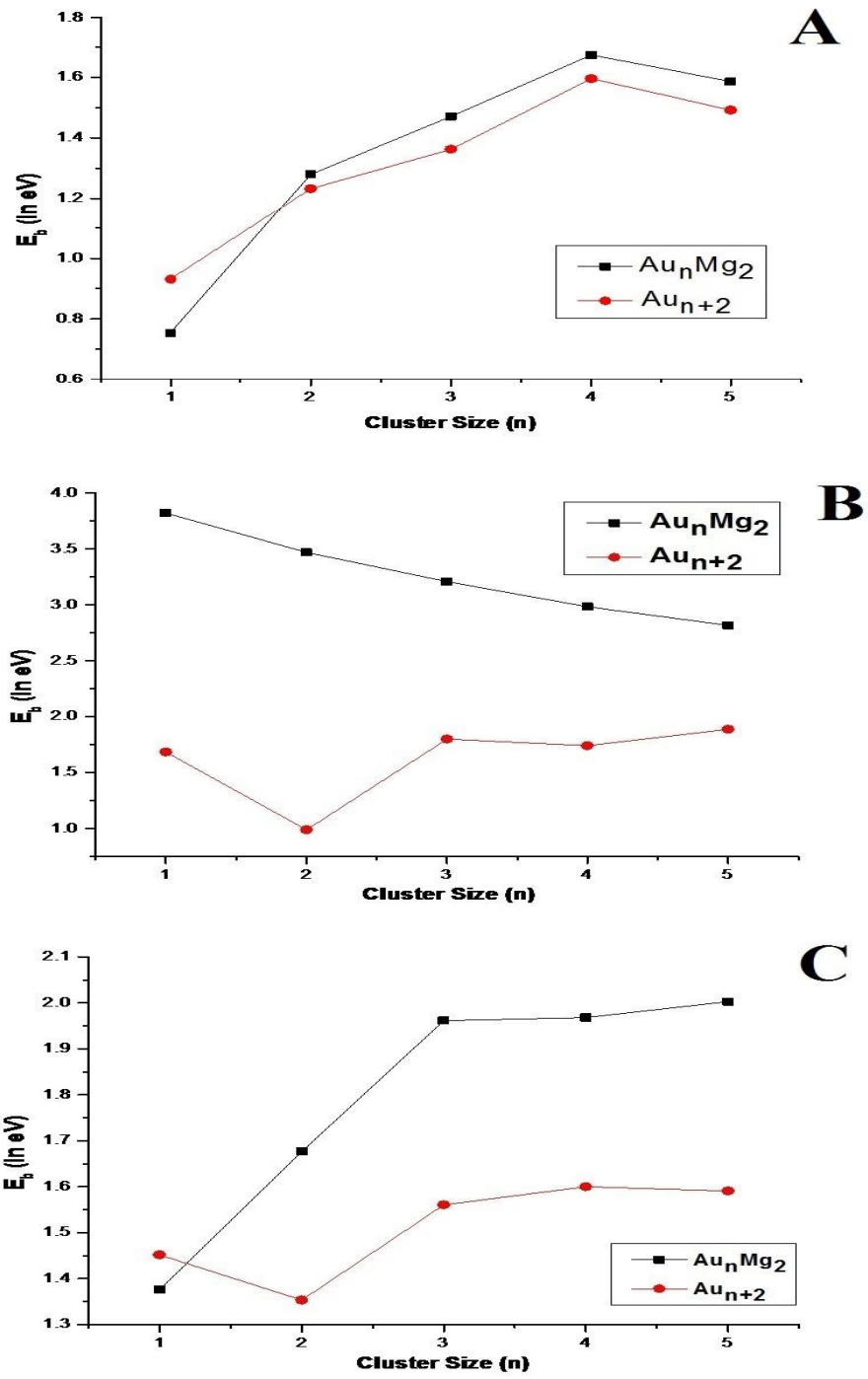

Figure 3.2.4 Variation of binding energies with respect to cluster size for (A) neutral, (B) cationic and (C) anionic clusters in bare and magnesium doped gold clusters.

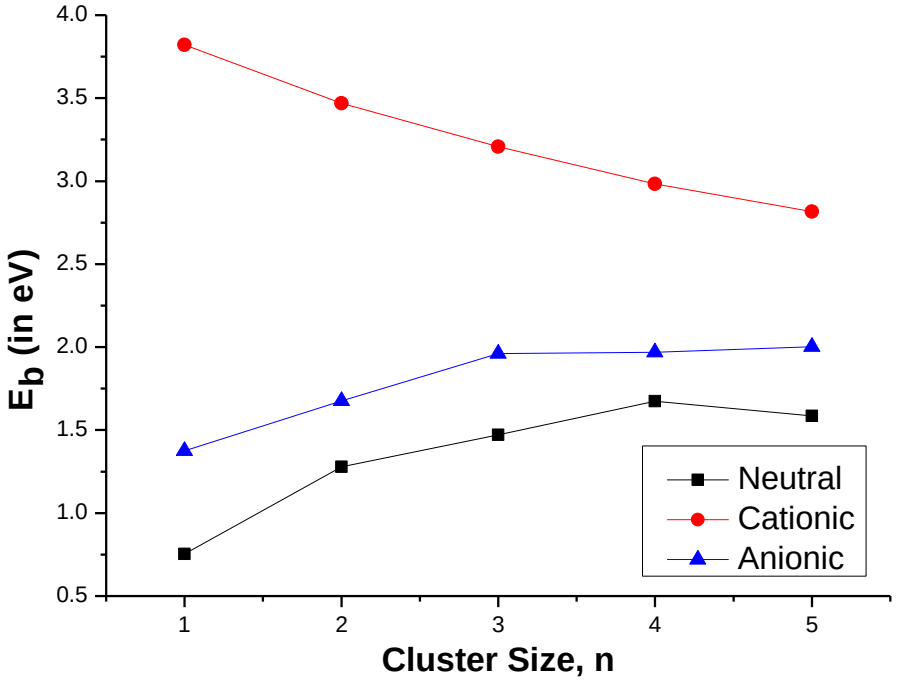

Figure 3.2.5 Comparison of binding energy per atom among charge and neutral clusters of Au_nMg_2 clusters.

3.2.3.2.2 Fragmentation energies

Figure 3.2.6 shows the variation of values of fragmentation energies for the most stable isomers as a function of cluster size. From the figure it can be seen that both bare as well as doped clusters exhibit even-odd alternation with respect to cluster size. For neutral bare clusters, the clusters with even number of atoms are more stable than that with odd number of atoms. However, the reverse is observed for the charged clusters and the clusters having odd number of atoms are more stable. The neutral and anionic Au_nMg_2 clusters follow same trend as observed for bare clusters and the plot for anionic cluster is similar to that obtained in previous study [28]. For neutral clusters, a sharp peak occurs at n=4 whereas for cationic and anionic clusters, sharp peaks occur at n=2 and n=3 respectively resulting the stability of these clusters in the region n=1-5.

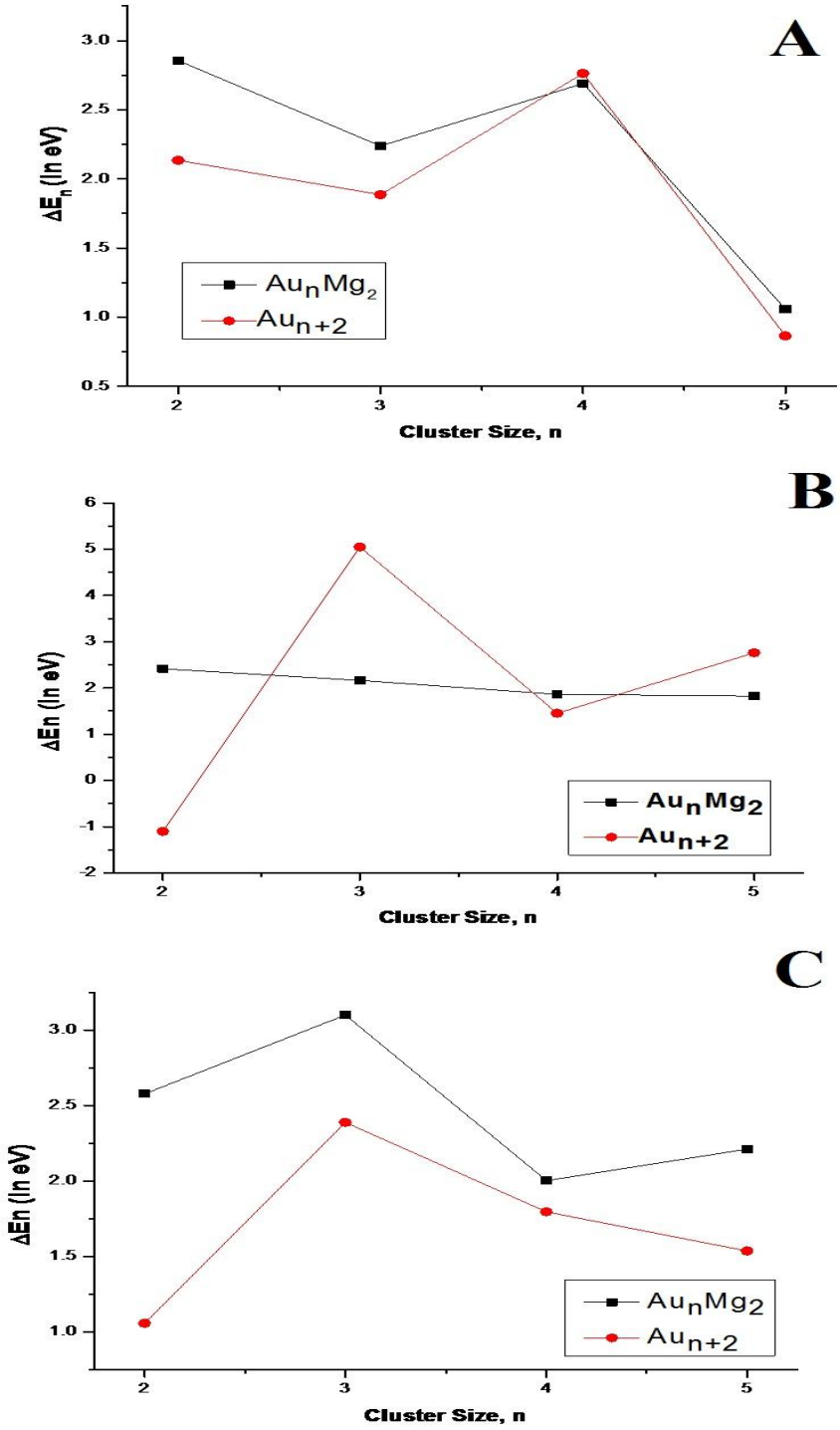

Figure 3.2.6 Variation of fragmentation energies with respect to cluster size for (A) neutral, (B) cationic and (C) anionic clusters in bare and magnesium doped gold clusters.

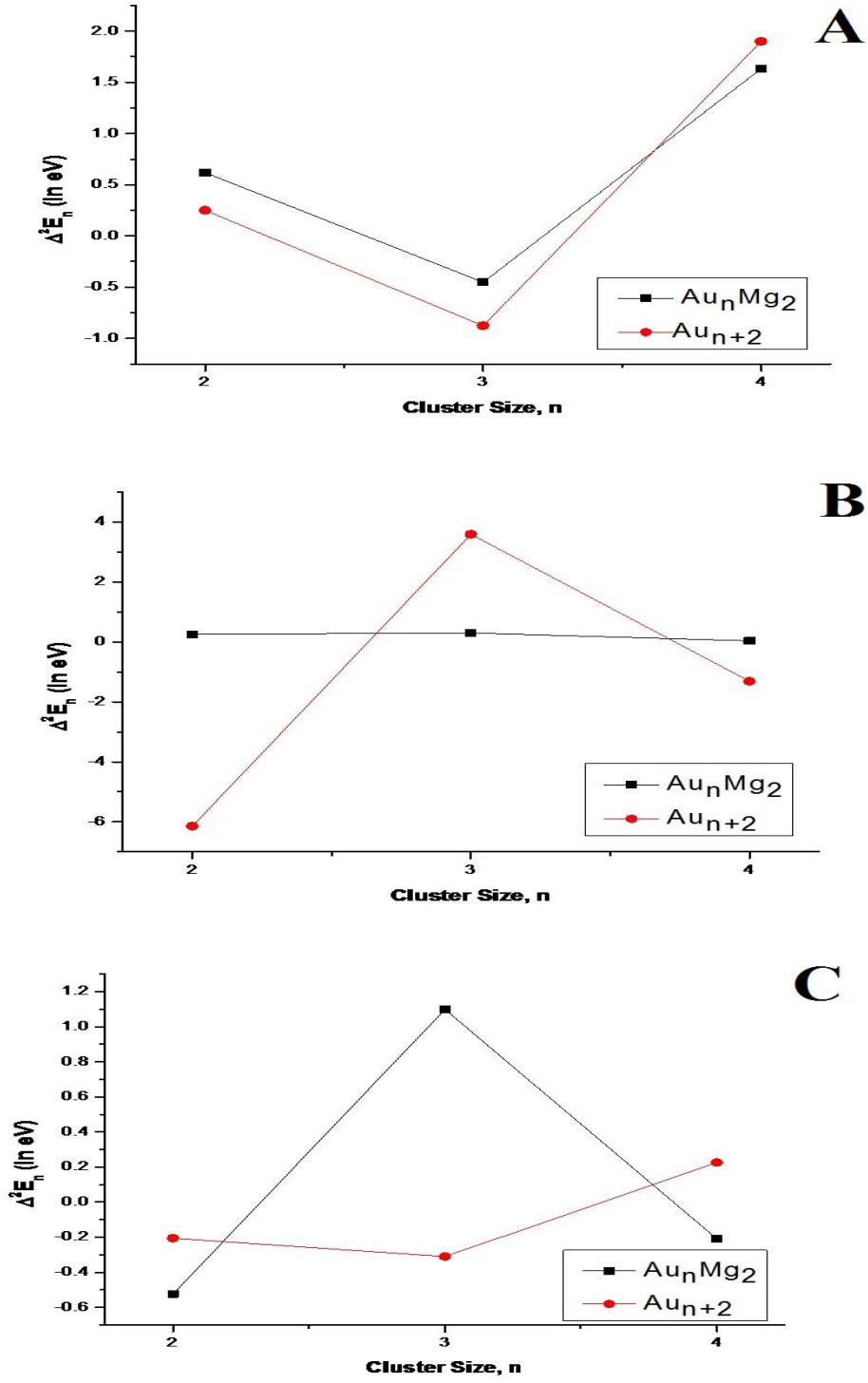

Figure 3.2.7 Variation of second order difference of energies with respect to cluster size for (A) neutral, (B) cationic and (C) anionic clusters in bare and magnesium doped gold clusters.

3.2.3.2.3 Second-order difference of energies

The second-order difference of energies, (Δ^2E), provides the relative stability of a cluster of size n with respect to its neighbor. Figure 3.2.7 provides the variation of values of fragmentation energies for the most stable isomers as a function of cluster size. The figure clearly indicates the even-odd alternation for both bare and doped clusters. For neutral doped clusters, the cluster with n=4 shows a sharp peak indicating its higher stability. Similarly, n=2 and n=4 tend to have greater stability for cationic and anionic clusters, respectively.

3.2.3.3 Ionization potential and Electron affinity

Using the same level of theory, we have calculated the vertical electron affinity (VEA) vertical ionization potential (VIP) and adiabatic ionization potential (AIP) values of the pure and doped clusters.

VEA measures the energy difference between the neutral and the anion clusters when the anion is at the optimized geometry of the neutral cluster. Thus,

$$VEA = E_{(\text{optimized neutral})} - E_{(\text{anion at optimized neutral geometry})} \quad (3.2.1)$$

Ionization potential (IP) measures the energy difference between the ground state of the neutral and the ionized clusters. If the ionized cluster has the same geometry as the ground state of the neutral, the ionization energy corresponds to the vertical ionization potential (VIP). On the other hand, the energy difference between the ground state of the cation and ground state of the neutral is referred to as the adiabatic ionization potential (AIP). VIP is generally calculated by using the following formula

$$VIP = E_{(\text{cation at optimized neutral geometry})} - E_{(\text{optimized neutral})} \quad (3.2.2)$$

Similarly, AIP is calculated as:

$$AIP = E_{(\text{optimized cation})} - E_{(\text{optimized neutral})} \quad (3.2.3)$$

The calculated VEA values for the pure and Al doped clusters are listed in Table 3.2.1. The values are in the range 2.02 to 3.56 eV for the pure clusters and 1.26 to 2.59 eV for the doped clusters. These values obtained for Au_n clusters are in the close range of the

previous experimental results [34]. The plot of VEA against cluster size is depicted in Figure 3.2.8. From the figure, we can see that the values of VEA are for each cluster show an obvious oscillating behavior with the increasing cluster size. The even number clusters have lower VEA values compared to the odd ones and hence are most stable. The VEA values for the doped clusters also have low VEA values indicating that they are more stable than the pure clusters. We are not able to compare the VEA values of Au_nMg_2 clusters due to lack of experimental values.

Table 3.2.1 Vertical electron affinities of neutral Au_{n+2} and Au_nMg_2 clusters (n=1-5)

	Au_{n+2}		Au_nMg_2
n	VEA (in eV)	Experimental [34]	VEA (in eV)
1	3.56	3.88	1.39
2	2.48	2.75	1.26
3	2.99	3.09	2.03
4	2.02	2.13	1.67
5	2.69	3.46	2.59

The VIP and AIP values obtained for Au_n and Au_nMg_2 are provided in Table 3.2.2. The values obtained for Au_n are in good agreement with the previous experimental results [35]. Due to lack of experimental values, we are not able to make direct comparison on the doped clusters. The plot of VIP values with respect to cluster size (Figure 3.2.9) shows even-odd alternation and indicates that the values obtained for odd numbered clusters are lower than that of their even counterparts. Therefore, even clusters are more stable than the odd ones. The value of VIP for Au_4Mg_2 is -7.88 eV which is highest among all the clusters. Hence it is the most stable cluster.

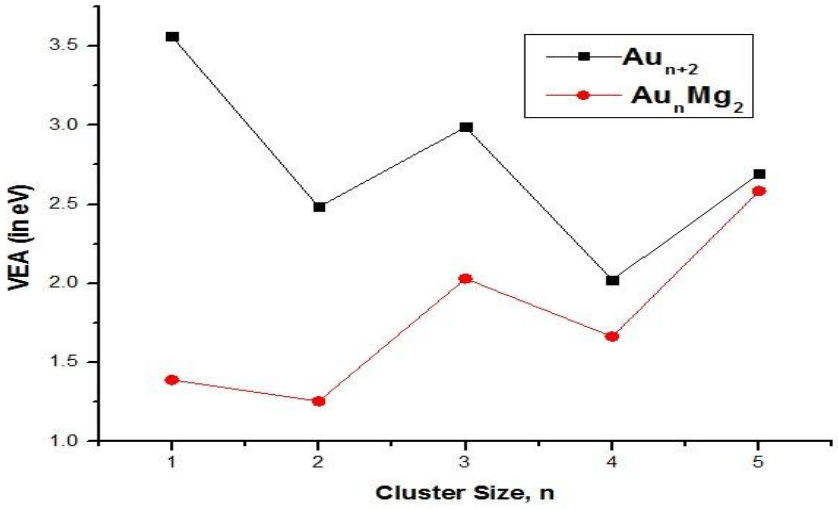

Figure 3.2.8 Variation of VEA values with respect to cluster size for pure and Mg doped Au clusters.

Table 3.2.2 Vertical and adiabatic ionization potentials of neutral Au_{n+2} and Au_nMg_2 clusters (n=1-5)

	Au_{n+2}			Au_nMg_2	
n	VIP (in eV)	AIP (in eV)	Experimental [35]	VIP (in eV)	AIP (in eV)
1	6.99	6.99	7.27	5.84	5.84
2	7.81	10.2	8.60	6.28	6.28
3	7.06	7.06	7.61	6.36	6.36
4	8.38	8.38	8.80	7.88	7.19
5	6.48	6.48	7.80	6.43	6.43

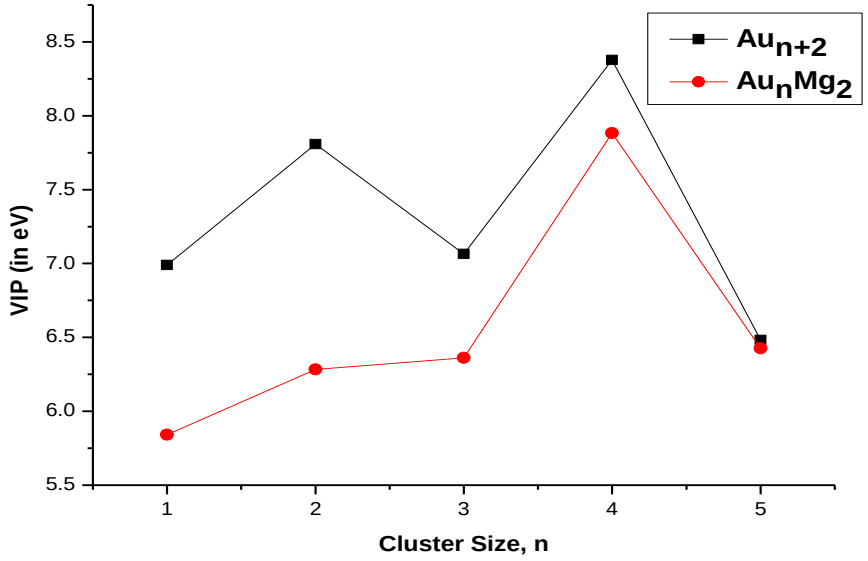

Figure 3.2.9 Variation of VIP values with respect to cluster size for pure and Mg doped Au clusters.

3.2.3.4 QTAIM analysis

To study the topology of electron density, we have used Bader's quantum theory of atoms in molecules (QTAIM) [19-21]. The parameters we have used here to ascertain the nature and extent of bonding between two atoms are the electron density, ρ and the Laplacian of electron density, $\nabla^2\rho$ at the bond critical point (BCP). The presence of BCP in all the clusters indicates the interaction between the Au and Mg atoms. The most stable isomers that are found during geometry optimization are taken QTAIM analysis, we. The focus of this QTAIM study is to notice the type of bond involves and the variation of bonding on doping Mg in Au clusters. The different values of the two parameters that we observed during QTAIM are provided in Table 3.2.3 for most stable bare and doped clusters.

Table 3.2.3 Electron density, ρ and the Laplacian of electron density, $\nabla^2\rho$ at the bond critical points (BCP) for some selected clusters.

Cluster	Interaction	ρ	$\nabla^2\rho$
Neutral			
Au_3	Au1 - Au2	0.06	0.15
	Au1 - Au3	0.06	0.15
Au_4	Au2 - Au4	0.06	0.15
	Au1 - Au2	0.05	0.12
	Au2 - Au3	0.05	0.12
	Au1 - Au4	0.05	0.12
$AuMg_2$	Mg1 - Au3	0.03	0.07
	Mg2 - Au3	0.03	0.07
Au_2Mg_2	Mg1 - Au3	0.03	0.1
	Mg2 - Au3	0.03	0.1
	Mg1 - Au4	0.03	0.1
	Mg2 - Au4	0.03	0.1
Cationic			
Au_3	Au1 - Au2	0.06	0.13
	Au1 - Au3	0.06	0.13
	Au2 - Au3	0.06	0.13
Au_4	Au2 - Au4	0.05	0.12
	Au1 - Au2	0.05	0.12
	Au2 - Au3	0.05	0.12
	Au1 - Au4	0.05	0.12
	Au3 - Au4	0.05	0.12
$AuMg_2$	Mg1 - Au3	0.03	0.08
	Mg2 - Au3	0.03	0.08

Continued……

Cluster	Interaction	ρ	$\nabla^2\rho$
Au_2Mg_2	Mg1 - Au3	0.03	0.11
	Mg2 - Au3	0.03	0.11
	Mg1 - Au4	0.03	0.11
	Mg2 - Au4	0.03	0.11
Anionic			
Au_3	Au1 - Au2	0.06	0.14
	Au1 - Au3	0.06	0.14
Au_4	Au2 - Au4	0.04	0.1
	Au1 - Au2	0.05	0.12
	Au2 - Au3	0.05	0.12
	Au1 - Au4	0.05	0.12
$AuMg_2$	Mg1 - Au3	0.02	0.06
	Mg2 - Au3	0.02	0.06
Au_2Mg_2	Au1 - Mg3	0.02	0.07
	Au2 - Mg3	0.02	0.07
	Au1 - Mg4	0.02	0.07
	Au2 - Mg4	0.02	0.07

The small and positive values obtained for ρ and $\nabla^2\rho$ for all the analysed structures in Table 3.2.3 indicates the covalent interaction between Au-Au and Au-Mg atoms. However, compared to that of Au-Au bond, bond critical point shifts towards Mg atom in Au-Mg bond as shown in Figure 3.2.10. The observation of basin paths for the some clusters from figure 3.2.11 clearly confirms the interaction between the Au-Au and Au-Mg atoms. The presence of ring critical points (RCP) in several clusters also support the cyclic structures that we obtained during optimisation. For example, we obtained a triangular structure for cationic Au_3 cluster. The QTAIM analysis confirms this structure by resulting the RCP as shown in A3 of Figure 3.2.11. Various smaller values of ρ and $\nabla^2\rho$ obtained for doped clusters compared to that of a pure clusters (Table 3.2.3) indicate the strong covalent bonding of the former one.

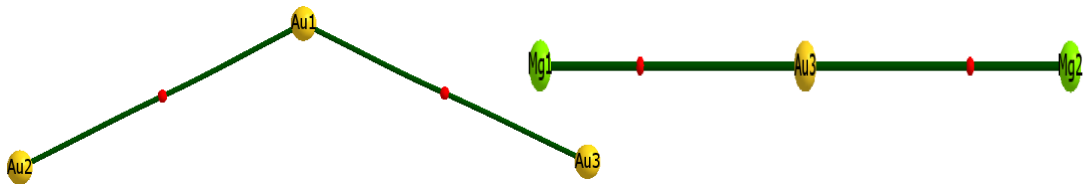

Figure 3.2.10 Shifting of BCP in Au-Au and Au-Mg bonds. The red dots indicate BCP.

3.2.3.5 Natural charge analysis

Applying the same level of theory, we have analysed the variation of charge for doping Mg atoms in Au clusters with the help of Mulliken atomic charge localization. The charge analysis results that in neutral $AuMg_2$ cluster, the Mg atoms have positive charges (0.477 e) whereas that of gold has negative charges (-0.954). Similarly, for the cationic $AuMg_2$ cluster, Mg atoms possess positive charges (1.041) and Au atoms has negative charge (-1.083). In case of anionic $AuMg_2$ clusters, the charges are 0.048 and -1.096 for Mg and Au atoms, respectively. Hence charges are transfered from Mg atom to Au atom which may arise due to larger electronegativity of Au (2.54) as compared to Mg (1.31). The HOMO-LUMO isosurfaces are also generated for Au_3 and $AuMg_2$ as shown in Figure 3.2.12.

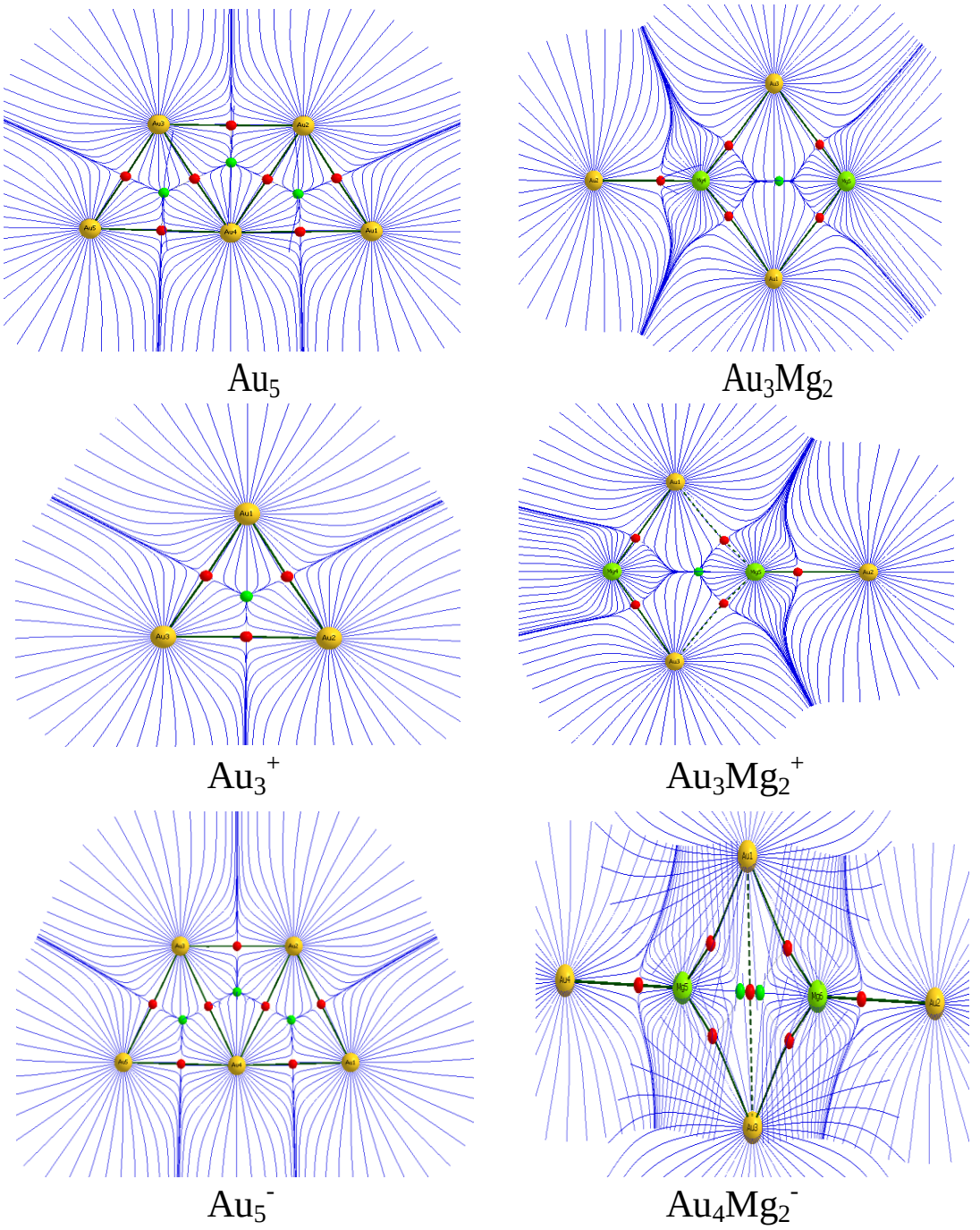

Figure 3.2.11 Trajectory field in some of the Au_n and Au_nMg_2 clusters. Gold and magnesium atoms are represented by yellow and green spheres respectively. Bond paths and basin paths are indicated by dark green and blue lines, while the interatomic surfaces are indicated by dark blue lines. Red and green dots indicate bond critical points and ring critical points, respectively.

The isosurfaces clearly indicate the formation of π-bonds in both the cases by sidewise overlapping and it support the formation of covalent bond in accordance with the QTAIM study.

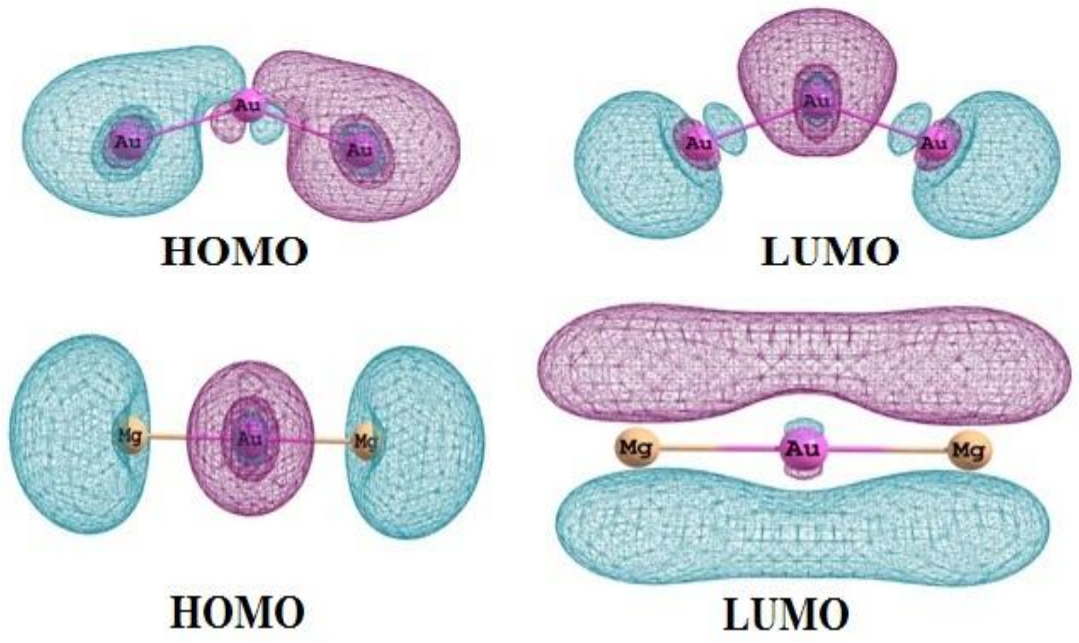

Figure 3.2.12 HOMO and LUMO isosurfaces of Au_3 and $AuMg_2$ clusters.

3.2.4 SALIENT OBSERVATIONS

We have presented a systematic study of the structures, stabilities and electronic properties of small bare gold clusters Au_n and bimetallic complexes of doubly Mg doped Au_nMg_2 (charged as well as neutral) using PW91PW91 level of theory. The study results the following observations:

1. Almost all the Mg doped Au_n clusters adopt plannar structures. The structures of doped clusters are different to that of pure clusters indicating the effect of doubly doped mg in the Au clusters.
2. The relative stabilities as a function of cluster size are explained with binding energy per atom, fragmentation energies and second-order difference of energies. These curves show even-odd oscillory behaviours and results reveal that Au_6, Au_5^+, Au_6^-, Au_4Mg_2, $Au_2Mg_2^+$, $Au_3Mg_2^-$

structures have enhanced chemical stabilities. The stability trends clearly indicates that doped clusters are more stable to that of bare clusters.

3. Ionization potentials and electron affinities of Au_n and Au_nMg_2 clusters are discussed and compared with experimental results. Our theoretical results are found to be in good agreement with experimental values. Consequently, our obtained atomic structures of Au_nMg_2 clusters should be reliable.
4. The QTAIM study results that the electron density, ρ , and its Laplacian, $\nabla^2\rho$ at the Au–Au and Au–Mg BCPs are very small and positive. These two parameters confirm the presence of covalent interactions in the studied clusters.
5. The natural charge analysis confirms the transfer of charge from Mg to Au atoms. The covalent behaviour is also supported by HOMO-LUMO isosurfaces. Therefore, as a whole we can suggest that doping of doubly doped Mg can increase the stability of the pure Au clusters.

3.3 EFFECT OF DOUBLE ALUMINIUM DOPING ON SMALL GOLD CLUSTERS

3.3.1 INTRODUCTION

Aluminium is a member of boron family and third most abundant element as well as most abundant metal in the earth. Recently, the study of the geometric and electronic properties of nanoclusters composed of Au and Al atoms finds importance both for theoretical reasons and for their potential applications in the field of nanotechnology. A few studies on aluminium doped gold clusters have been already carried out till date. Bouwen *et al.* produced bimetallic Au_nAl_m clusters by a dual-target dual-laser vaporization source [36]. They differenciate different bimetallic clusters in terms of different cluster geometries dependent on the nature of the dopant atoms. Using DFT, Wang *et al.* performed theoretical study on anioinic Au_nAl^- ($1 \leq n \leq 8$) clusters [37]. Simillarly Zhao *et al.* studied the Au_nAl (n=1-13) clusters [38] and Majumdar *et al.* investigated the Au_5Al clusters [27]. These study reveals that doping of single Al can effect the stability and structural properties of bare Au clusters.

If we consider the double Al doped gold clusters, to the best of our knowledge, no systematic theoretical investigations into Al_2Au_n clusters have been performed. Therefore it is both natural and promising for us to investigate the properties of doubly Al doped Au clusters. Therefore, by applying DFT we have studied the structural and electronic properties of neutral as well as charged Au clusters doped with two Al atoms, Au_nAl_2 (n=1-5). The importance of this work lies in the fact that nanosized Au clusters already shows tremendous catalytic activity for different types of reactions and doping of a metal like Al can further enhanced its catalytic property. The novelity of the work with reference to the previous works lies in the facts that for the first time we have studied the all neutral and charged clusters for two Al metal doped Au clusters and compared with the pure ones. Also for the first time, we have performed QTAIM study in the Al doped Au clusters to study the bond parameters. Therefore, our present study can provide powerful platform to consider the Al doped Au clusters in the further experimental research.

3.3.2 COMPUTATIONAL DETAILS

The initial structures in neutral state have been generated using classical simulated annealing method with the help of Forcite Plus code as encoded in the MATERIAL STUDIO software [29]. The Universal force field (UFF) [30] which is already proved to be reliable for gold based systems [31,32] has been adopted to perform this simulation. The cut-off radius is chosen to be 15.5 Å and a NVE ensemble is used. A total of 100 annealing structures are generated at high temperature (1000 K) and 50 heating ramps per cycle. The most stable structures obtained by this simulation is used as the input for further DFT calculations.

Geometry optimizations and frequency analysis of Au_nAl_2 clusters are carried out using DFT based gradient-corrected exchange and correlation functional of Perdew-Wang (PW91PW91) [33] to explore the stationary points on the potential energy surface. This functional already give reliable results for previous studies on Al doped Au clusters [37,38]. To consider the relativistic effects of Au, we have used the Los Alamos LANL2DZ [15,16] Effective Core Pseudopotentials (ECP) and valence double-ζ basis sets for Au. The Al atoms are treated with 6–311+G(d) basis set. Full geometry optimizations have been performed for the neutral and charged clusters without imposing any symmetry constraints. In order to obtain the lowest energy doped isomers, initial structures were constructed substituting Au atoms by Al atoms in the pure gold structures at various attaching sites. The vibrational frequencies for all the structures are found to be positive confirming them to be at energy minima. The zero-point vibrational energy corrections have been included in all the calculations. All the calculations are carried out using GAUSSIAN 09 suits of program [12]. The total energies of the most stable clusters are used to determine their binding energy, relative stability, ionization potential as well as electron affinity as a function of clusters size to describe the stability and electronic properties of the clusters. The nature of bonding in the clusters were also studied by QTAIM method with the help of AIMALL package [22].

3.3.3 RESULTS AND DISCUSSION

3.3.3.1 Structural study of Au_nAl_2 clusters

The various lowest energy structures for neutral and charged Au_n and Au_nAl_2 clusters are shown in Figures 3.3.1-3.3.3. Among various isomers obtained for a particular cluster, the energy of the most stable isomer is taken as zero and energy of the others are compared relative to it.

3.3.3.1.1 Neutral clusters

The optimized structures for neutral clusters are depicted in Figure 3.3.1. The bare Au clusters have been optimized first which are in good agreement with the previous study [23]. Moving to the doped clusters, the most stable cluster for $AuAl_2$ is 1(1a) having triangular shape. The calculated Au-Al bond length here is 2.545 Å which is in accordance with previous study on Al doped gold clusters(2.419 Å) [38]. The other isomer 1(1b) is higher in energy compared to 1(1a) by 0.51eV. For Au_2Al_2, the lowest energy isomer is 1(2a) having sqare plannar geometry and Au-Al bond length of 2.637 Å. The other isomer is found to be higher in energy by 0.18 eV. In case of Au_3Al_2, e the most stable isomer is 1(3a) having shortest Au-Al bond length of 2.413 Å. For Au_4Al_2, the most stable isomer is 1(4a) having shortest Au-Al bond length of 2.412 Å. Finally, for Au_5Al_2 cluster we obtained a stable isomer 1(5a) having the same geometry as the bare counterpart. Here the shortest Au-Al bond length is found to be 2.506 Å.

This study on neutral doped clusters points out that all the isomers have planar structure. This is in contrast to the study on single Al doped Au clusters [38,39] where 3D isomers are observed in most of the clusters. Instead of n=2 and 5, all the most stable isomers for double Al doped clusters have different geometries compared to the pure clusters.

3.3.3.1.2 Charged Clusters

The optimized structures for the cationic and anionic clusters are shown in Figure 3.3.2 and 3.3.3. For cationic $AuAl_2^+$ clusters, we get only one isomer 2(1a) by

replacing the Au atoms with Al atoms at different positions. The isomer is found to be bent in shape with Au-Al bond length of 2.604 Å.

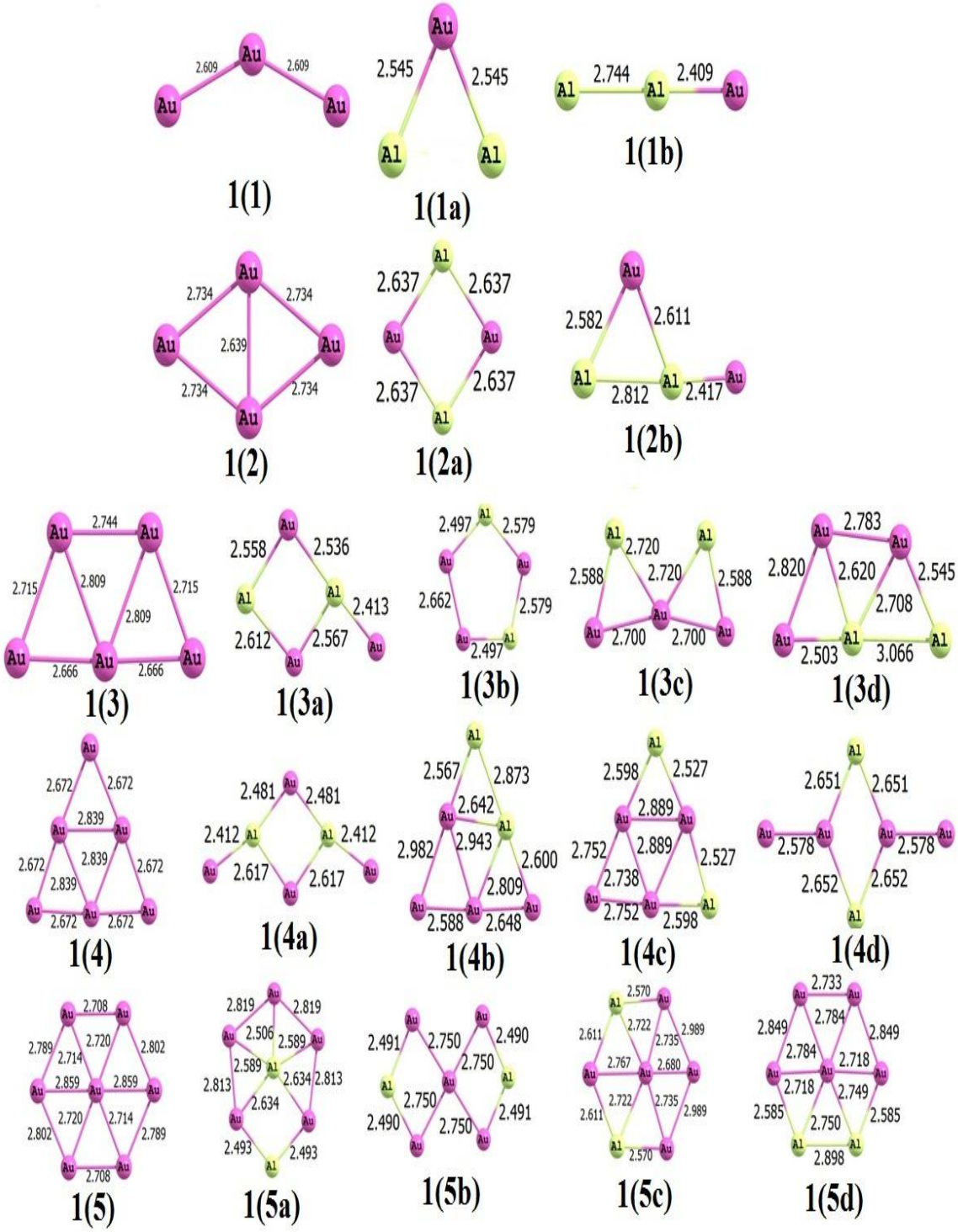

Figure 3.3.1 Optimized structures of neutral Au_{n+2} and Au_nAl_2 (n = 1–5) clusters

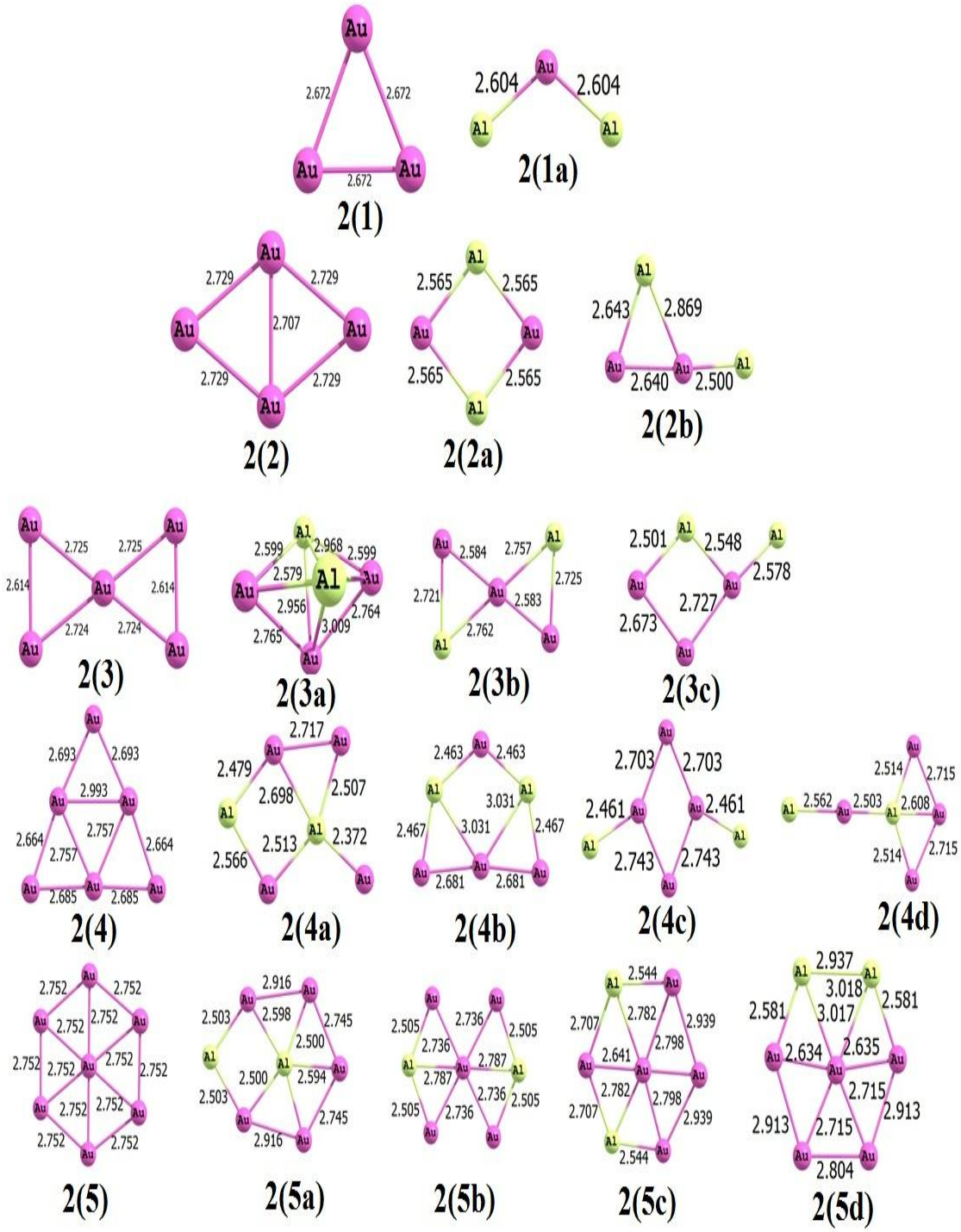

Figure 3.3.2 Optimized structures of cationic Au_{n+2} and Au_nAl_2 (n = 1–5) clusters

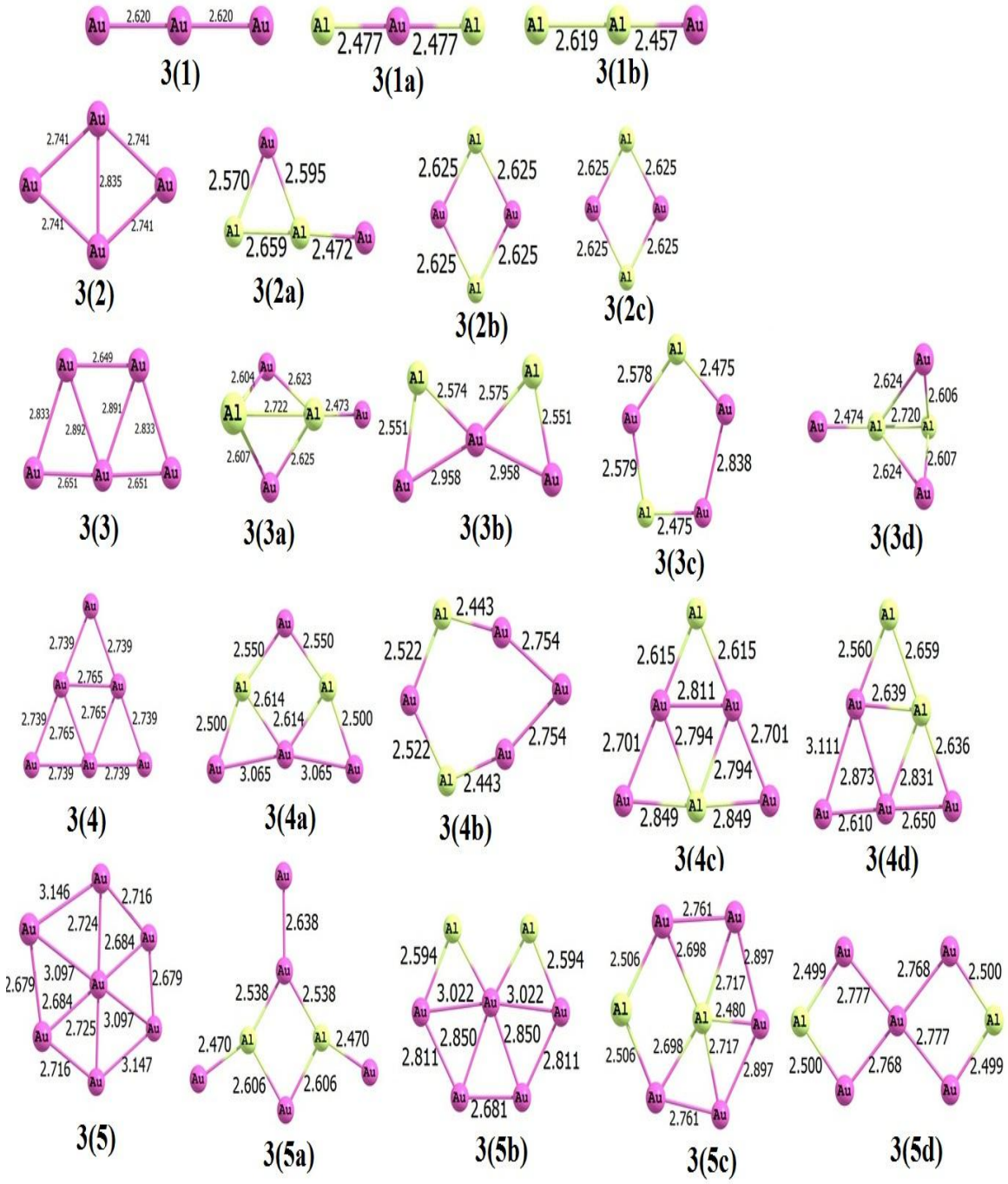

Figure 3.3.3 Optimized structures of anionic Au_{n+2} and Au_nAl_2 (n = 1–5) clusters

For $Au_2Al_2^+$ cluster, the most stable isomer is 2(2a) having the same square planner geometry. The other isomer 2(2b) is found to be higher in energy to 2(2a) by 0.74 eV. For the rest of the clusters, the lowest energy isomers are found to be 2(3a), 2(4a) and 2(5a) for $Au_3Al_2^+$, $Au_4Al_2^+$ and $Au_5Al_2^+$, respectively (Figure 3.3.2). A 3D isomer 2(3a) is obtained here for n=3 indicating a deviation from planarity of the clusters at this point. However, for the rest of the clusters, no any 3D isomer is observed. For anionic clusters, the most stable isomers are found to be 3(1a), 3(2a), 3(3a), 3(4a) and 3(5a) for $AuAl_2^-$, $Au_2Al_2^-$, $Au_3Al_2^-$, $Au_4Al_2^-$ and $Au_5Al_2^-$, respectively (Figure 3.3.3). For the most stable $Au_2Al_2^-$ cluster, the shortest Au-Al bond length of 2.472 Å is comparable with that of previous value of 2.48 Å as reported by Wang *et al.* [37]. For anionic clusters also a transition from 2D to 3D structure is observed at n=3.

This study on charged clusters shows that in contrast to neutral clusters, charged clusters posses a deviation from planarity. For the cationic clusters, apart from n=2 and 5, all the most stable isomers have different geometry to that of the bare clusters.

3.3.3.2 Stability of Au_nAl_2 clusters

The relative stabilities of the Au_nAl_2 clusters are calculated in terms of averaged binding energies per atom, (E_b) fragmentation energies, ΔE, and second-order difference of energies, $\Delta^2 E$, using formulae 3.1.1-3.1.7 (where M=Al).

3.3.3.2.1 Binding energies per atom

The variation of calculated binding energies per atom (E_b) for the most stable isomers as a function of cluster size is shown in Figure 3.2.4. The figure indicates that the binding energy per atom for pure clusters increases with cluster size for the neutral clusters which means that the clusters continue to gain energy during the growth process. For the charged clusters, the B.E. values show an even-odd alternation. In case of neutral and anionic doped clusters, the graphs show sharp peaks at n=4 and n=3, respectively, indicating the higher stability of these clusters in the region n=1-5. The E_b values decrease with cluster size for the cationic doped clusters. From the plots, it is clear that binding energy values for doped clusters are considerably higher than that of the pure clusters. It means that the doped clusters have greater stability in all the

neutral, cationic and anionic clusters in comparison to the bare Au counterparts. For neutral and anionic clusters, the variation of B.E. is found to be similar to that of the single doped clusters as reported earlier [37-39].

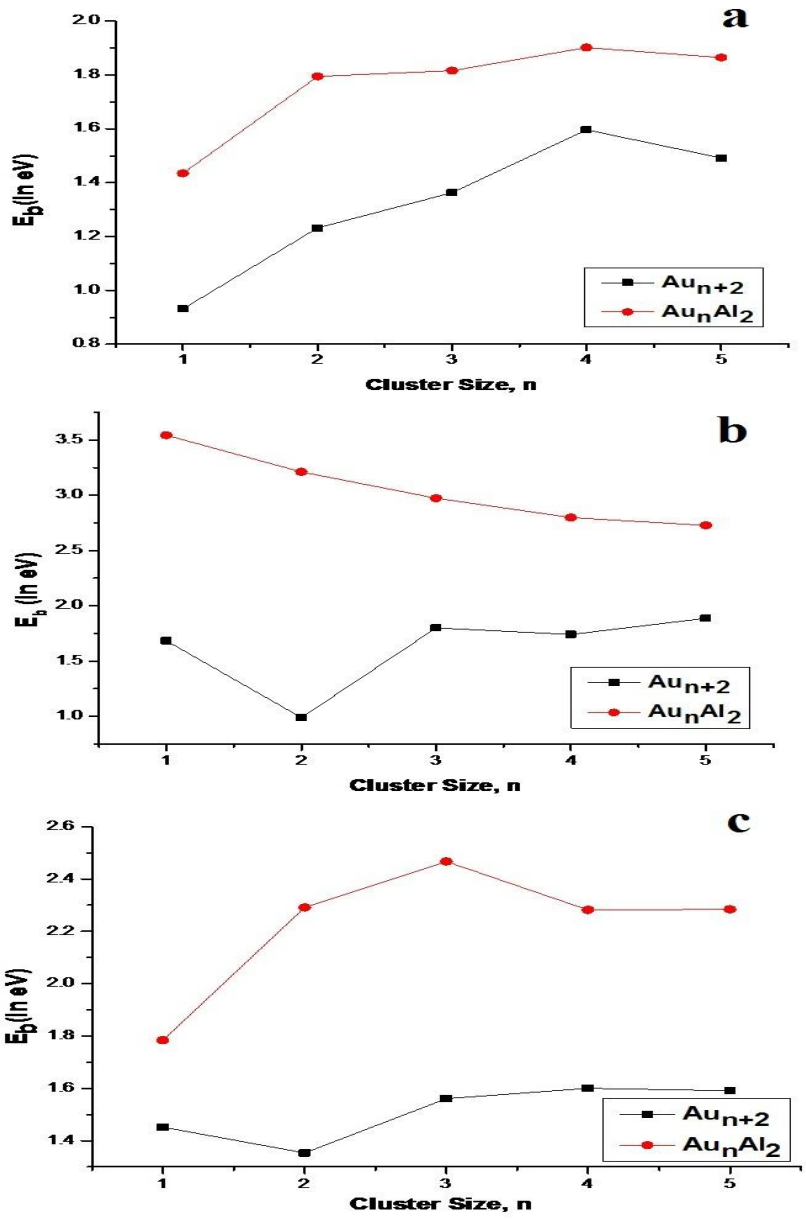

Figure 3.3.4 Variation of binding energies with respect to cluster size for (a) neutral, (b) cationic and (c) anionic clusters in bare and Al doped gold clusters.

On comparing the binding energies of charge and neutral clusters (Figure 3.3.5), the binding energy order is found to be increases as: neutral < anionic < cationic for Al doped clusters. This order is identical to that of our study on doubly Be and Mg doped Au clusters as reported in the previous two sub chapters.

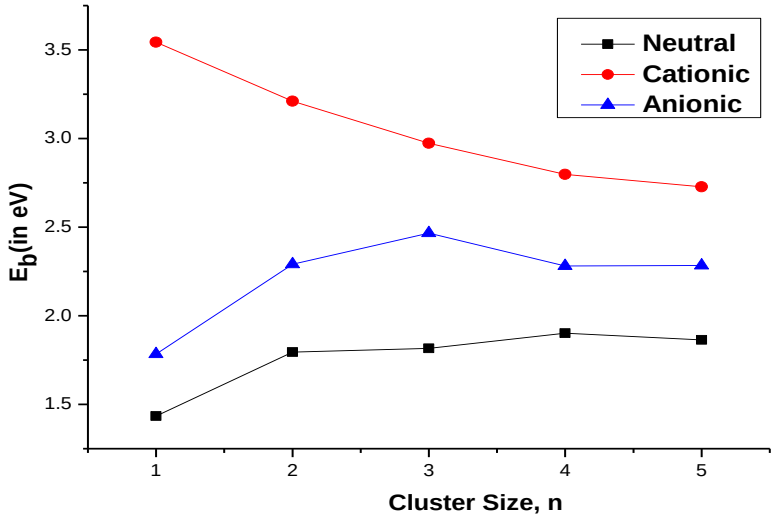

Figure 3.3.5 Comparison of binding energy per atom among charge and neutral clusters of Au_nAl_2 clusters

3.3.3.2.2 Fragmentation energies

The variation of values of fragmentation energies for the most stable Au and Al doped clusters as a function of cluster size are shown in Figure 3.3.6. From the figure we can see that both the bare as well as doped clusters exhibit even-odd alternation with respect to cluster size. For neutral clusters, $Au_{4,6}$ and $Au_{2,4}Al$ clusters have higher stability indicating that clusters with even number of atoms are more stable than that with odd number of atoms. However, for the charged clusters, the odd numbered clusters are seemed to be more stable. The neutral and anionic Au_nAl_2 clusters follow almost the same trend as observed for bare clusters. The variation of plots in these two types of clusters is identical with that of the previous study on singly doped clusters [38,39]. For neutral and anionic clusters, a sharp peak occurs at n=2 whereas for cationic clusters, sharp peaks occur at n=2 and 5 indicating the stability of these clusters in the region n=1-5.

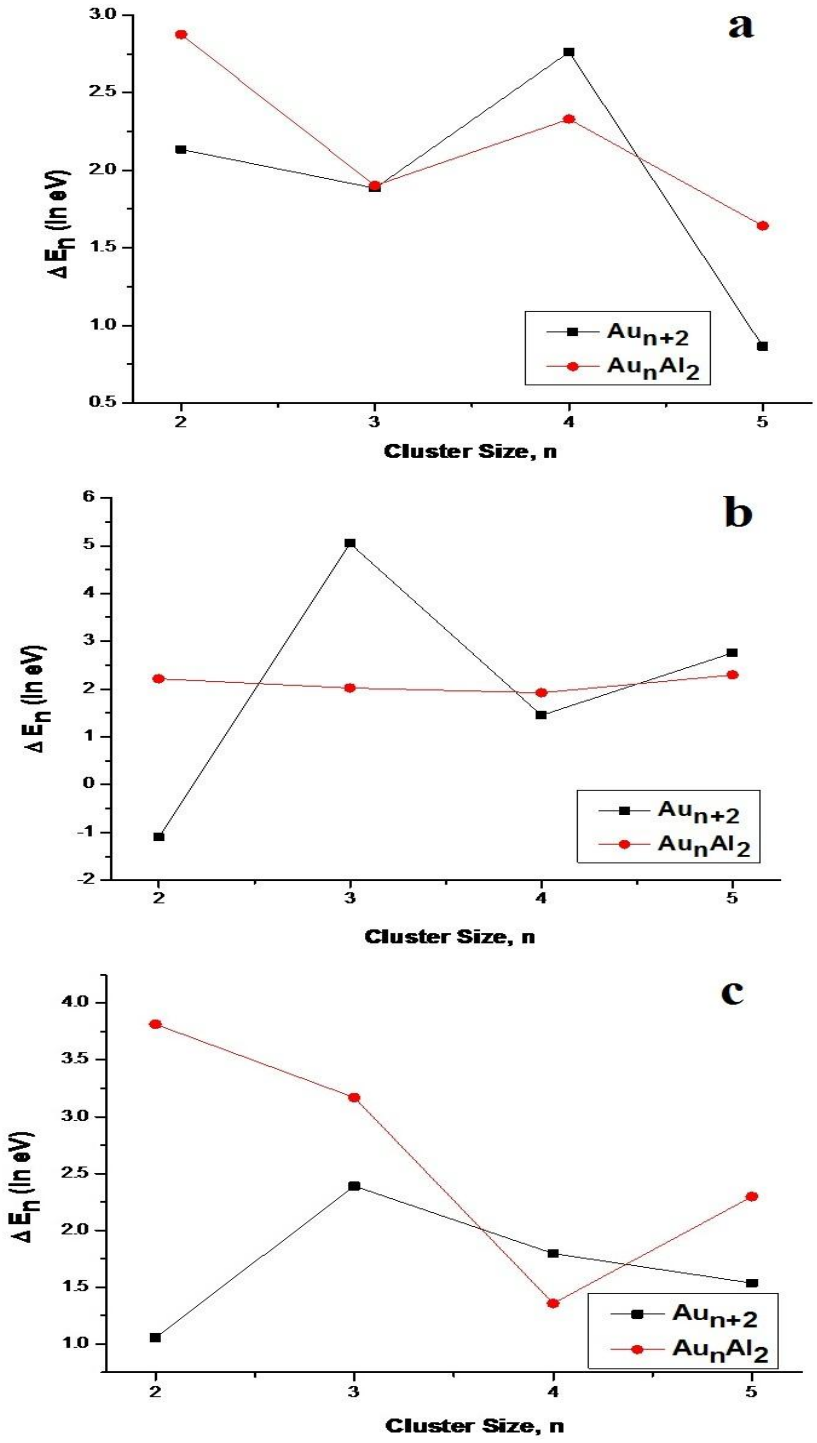

Figure 3.3.7 Variation of fragmentation energies with respect to cluster size for (a) neutral, (b) cationic and (c) anionic clusters in bare and aluminium doped gold clusters.

3.3.3.2.3 Second-order difference of energies

The variation of second-order difference of energies (Δ^2E) for the most stable Au and Al doped clusters as a function of cluster size is shown in Figure 3.3.7. From the figure it can be understand that both bare and doped clusters exhibit the even-odd alternation. For neutral clusters, the curve shows a peak at n=2 indicating its higher stability. In case of charged clusters, the curves show sharp peaks at n=2 and n=3 for cationic and anionic clusters respectively, indicating the stability of the clusters at these points. The variation of the plots for neutral and anionic clusters are found to be similar with that of singly Al doped Au clusters [38,39].

3.3.3.3 Ionization potential and Electron affinity

Using the same level of theory, we have calculated the vertical electron affinity (VEA) vertical ionization potential (VIP) and adiabatic ionization potential (AIP) values of the pure and doped clusters.

VEA, VIP and AIP of the clusters are calculated by using formula 3.2.1-3.2.3 of the previous section 3.2. The calculated values of VEA for the pure and Al doped clusters are provided in Table 3.3.1. The values are in the range 2.02 to 3.56 eV for the pure clusters and 1.13 to 2.44 eV for the doped clusters. The values obtained for Au_n clusters are in good agreement with previous experimental results [34]. The plot of VEA against cluster size is depicted in Figure 3.3.8. The figure indicates that the values of VEA for each cluster show an obvious oscillating behavior with the increasing cluster size. The even number clusters have lower VEA values compared to the odd ones and hence their stability is also high. The VEA values for the doped clusters have low VEA values indicating that they are more stable than the pure clusters. The variation of VEA with cluster size in this study seems to be identical with the previous results [38] as well. Due to lack of experimental values, we are not able to compare the VEA values of Au_nAl_2 clusters.

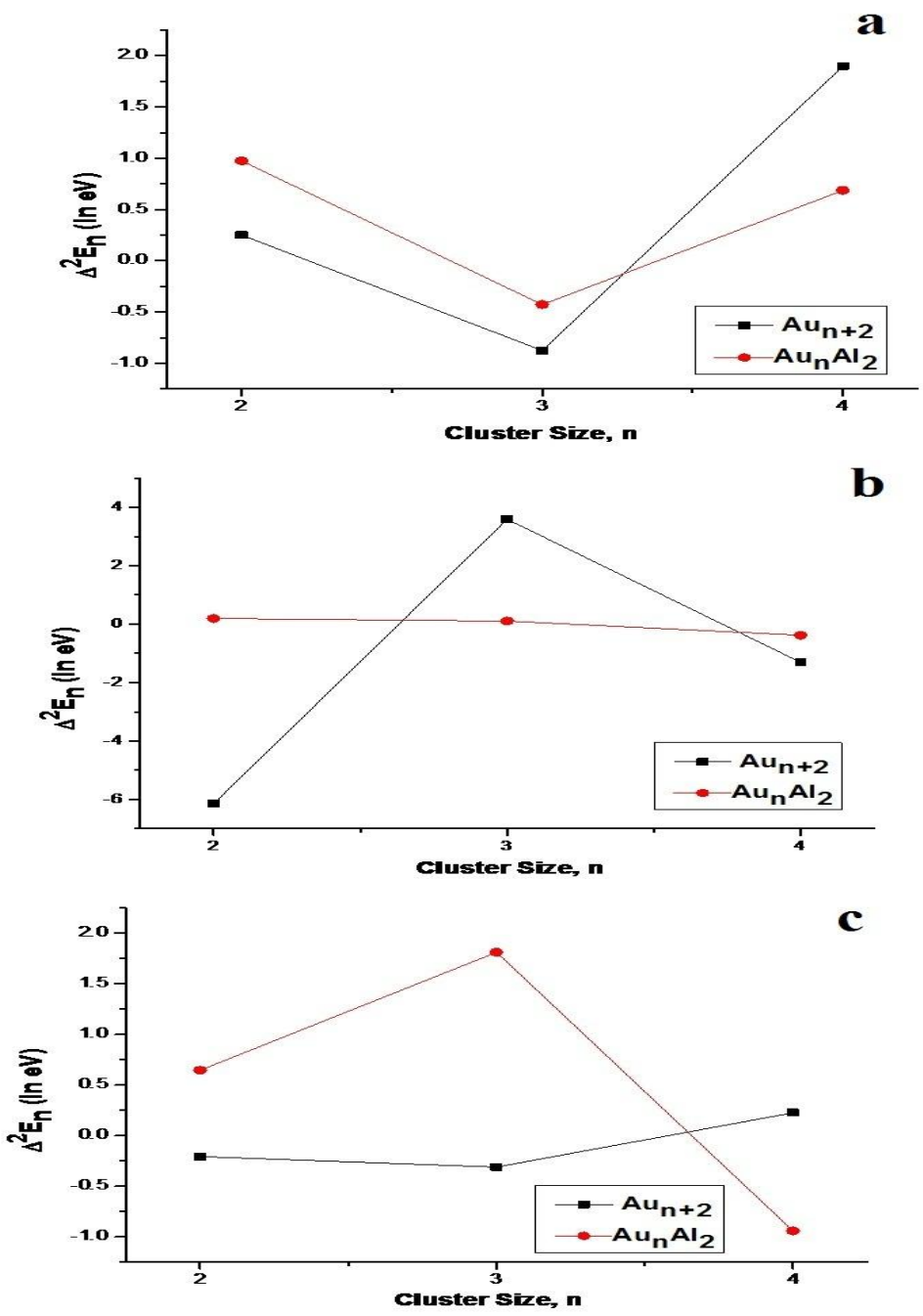

Figure 3.3.8 Variation of second order difference of energies with respect to cluster size for (a) neutral, (b) cationic and (c) anionic clusters in bare and aluminium doped gold clusters.

Table 3.3.1 Vertical electron affinities of neutral Au_{n+2} and Au_nAl_2 clusters (n=1-5)

	Au_{n+2}		Au_nAl_2
n	VEA (in eV)	Experimental [34]	VEA (in eV)
1	3.56	3.88	1.13
2	2.48	2.75	1.40
3	2.99	3.09	2.23
4	2.02	2.13	1.86
5	2.69	3.46	2.44

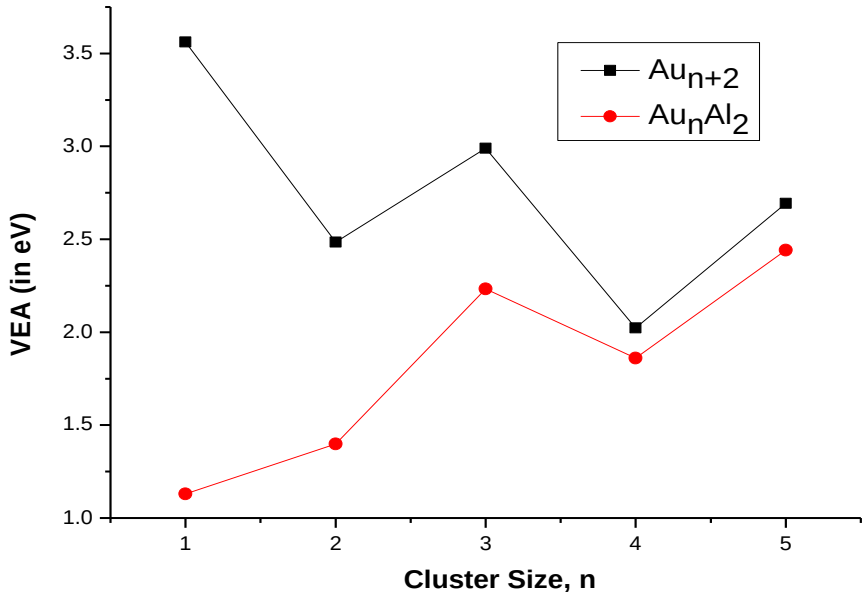

Figure 3.3.8 Variation of VEA values with respect to cluster size for pure and Al doped Au clusters.

Table 3.3.2 provides the calculated VIP and AIP values for Au_n and Au_nAl_2 clusters. The values obtained for Au_n clusters are in the range 6.48 to 8.48 eV which agrees well with the previous experimental results [35]. The direct comparison of the doped clusters is not possible due to the lack of previous results. The VIP values with respect to cluster size shows an even-odd alternation (Figure 3.3.9) with lower values for odd numbered clusters. Thus they are stability is less than the even numbered clusters. The calculations of VIP and VEA suggest that VIP values are larger than the VEA values for all the clusters. Hence these clusters can easily accept electrons.

Table 3.3.2 Vertical and adiabatic ionization potentials of neutral Au_{n+2} and Au_nAl_2 clusters (n=1-5)

	Au_{n+2}			Au_nAl_2	
n	VIP (in eV)	AIP (in eV)	Experimental [35]	VIP (in eV)	AIP (in eV)
1	6.99	6.99	7.27	5.87	5.87
2	7.81	10.20	8.60	6.54	6.54
3	7.06	7.06	7.61	5.75	6.41
4	8.38	8.38	8.80	6.50	6.82
5	6.48	6.48	7.80	6.18	6.16

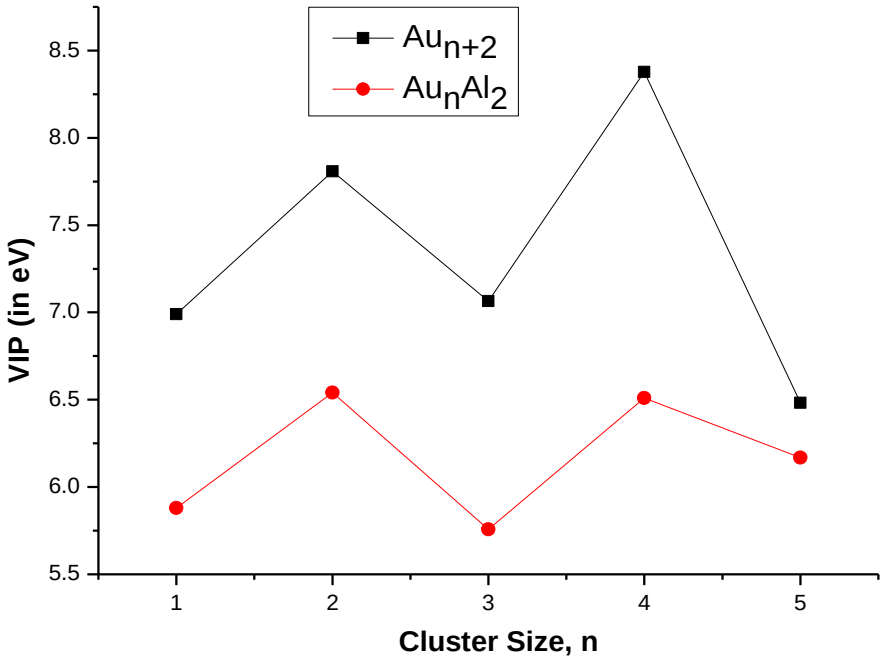

Figure 3.3.9 Variation of VIP values with respect to cluster size for pure and Al doped Au clusters.

3.3.3.4 QTAIM analysis

Bader's quantum theory of atoms in molecules (QTAIM) is also used here to study the topolgy of the clusters. The parameters used to ascertain the nature and extent of bonding here are the electron density, ρ and the Laplacian of electron density, $\nabla^2\rho$ at the bond critical point (BCP).

The presence of BCP in all the studied clusters indicates the interaction between the Au and Al atoms. We have considered only the most stable isomers that are found during geometry optimization in QTAIM analysis. The aim of this QTAIM study was to notice the type of bond involves and the variation of bonding on doping Al in Au clusters. The values of the two parameters that we observed during QTAIM are given in Table 3.3.3 for some selected clusters. The small and positive values obtained for ρ and $\nabla^2\rho$ for the structures in Table 3.3.3 indicates the covalent interaction between Au-Au and Au-Al atoms. Compared to the of Au-Au bond, bond critical point shifts towards Al atom in Au-Al bond as shown in Figure 3.3.10.

Table 3.3.3 Electron density, ρ and the Laplacian of electron density, $\nabla^2\rho$ at the bond critical points (BCP) for some selected clusters.

Cluster	Interaction	ρ	$\nabla^2\rho$
Neutral			
Au_3	Au1 - Au2	0.06	0.15
	Au1 - Au3	0.06	0.15
Au_4	Au2 - Au4	0.06	0.15
	Au1 - Au2	0.05	0.12
	Au2 - Au3	0.05	0.12
	Au1 - Au4	0.05	0.12
	Au3 - Au4	0.05	0.12
$AuAl_2$	Au1 - Al2	0.04	0.06
	Au1 - Al3	0.04	0.06
Au_2Al_2	Au1 - Al3	0.04	0.03
	Au2 - Al3	0.04	0.03
	Au1 - Al4	0.04	0.03
	Au2 - Al4	0.04	0.03
Cationic			
Au_3	Au1 - Au2	0.06	0.13
	Au1 - Au3	0.06	0.13
	Au2 - Au3	0.06	0.13
Au_4	Au2 - Au4	0.05	0.12
	Au1 - Au2	0.05	0.12
	Au2 - Au3	0.05	0.12
	Au1 - Au4	0.05	0.12
	Au3 - Au4	0.05	0.12
$AuAl_2$	Au1 - Al2	0.04	0.01
	Au1 - Al3	0.04	0.01

Continued……

Cluster	Interaction	ρ	$\nabla^2\rho$
Au_2Al_2	Au1 - Al3	0.04	0.04
	Au2 - Al3	0.04	0.04
	Au1 - Al4	0.04	0.04
	Au2 - Al4	0.04	0.04
Anionic			
Au_3	Au1 - Au2	0.06	0.14
	Au1 - Au3	0.06	0.14
Au_4	Au2 - Au4	0.04	0.1
	Au1 - Au2	0.05	0.12
	Au2 - Au3	0.05	0.12
	Au1 - Au4	0.05	0.12
	Au3 - Au4	0.05	0.12
$AuAl_2$	Au1 - Al2	0.04	0.07
	Au1 - Al3	0.04	0.07
Au_2Al_2	Au1 - Al3	0.05	0.08
	Au2 - Al3	0.04	0.03
	Au2 - Al4	0.04	0.06
	Al3 - Al4	0.03	0.06

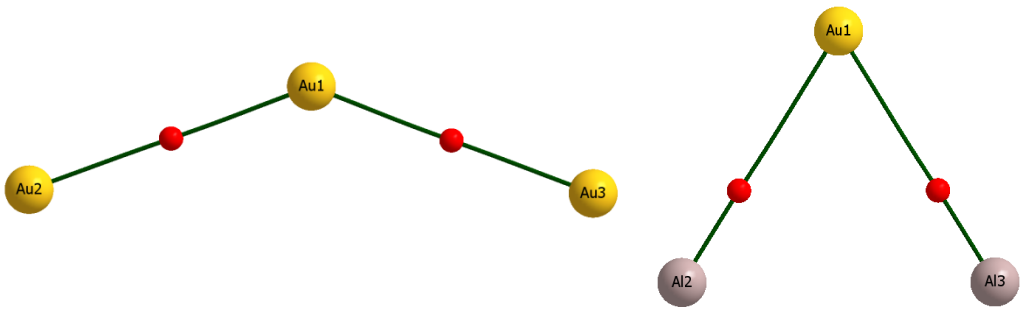

Figure 3.3.10 Shifting of BCP in Au-Au and Au-Al bonds. The red dots indicate BCP.

From Table 3.3.3 we can see that the ρ and $\nabla^2\rho$ values for the doped clusters are smaller than that of the pure clusters indicating that extent of covalency is stronger in the doped clusters.

To further study the interaction between Au and Al atoms, we observed the basin paths of the clusters and provided them in Figure 3.3.11. The basin paths clearly confirm the interaction between the Au-Au and Au-Al atoms. The cyclic structures obtained during optimization are also confirmed by the presence of ring critical points(RCP) as observed during QTAIM study. For example we obtained a cyclic structure containing several rings for neutral Au_6 cluster which is confirmed by the presence of 4 RCPs (Figure 3.3.11). Thus our QTAIM analysis results that the studied clusters mainly possess covalent characters which is higher for the doped clusters.

3.3.3.5 Natural Charge Analysis

We have analysed the variation of charge for doping Al atoms in Au clusters with the help of Mulliken atomic charge localization applying the same level of theory,. The charge analysis reveals that Al atoms has positive charges (0.441 e) whereas that of gold has negative charges (-0.881) in neutral $AuAl_2$ cluster. For the cationic $AuAl_2$ cluster, Al atoms possess positive charges (0.966) and Au atoms has negative charge (-0.932). Simillarly, for anionic $AuAl_2$ cluster, charges are 0.114 and -1.229 for Al and Au atoms, respectively. These charge values indicates the transfer of charges from Al atom to Au atom which may be due to the larger electronegativity of Au (2.54) as compared to Al (1.61). We have Also generated the HOMO-LUMO isosurfaces for neutral Au_3 and $AuAl_2$ as shown in Figure 3.3.12. The isosurfaces clearly confirms the formation of covalent bonds in all the three types of clusetrs. This fact support the formation of covalent bond in accordance with our QTAIM study.

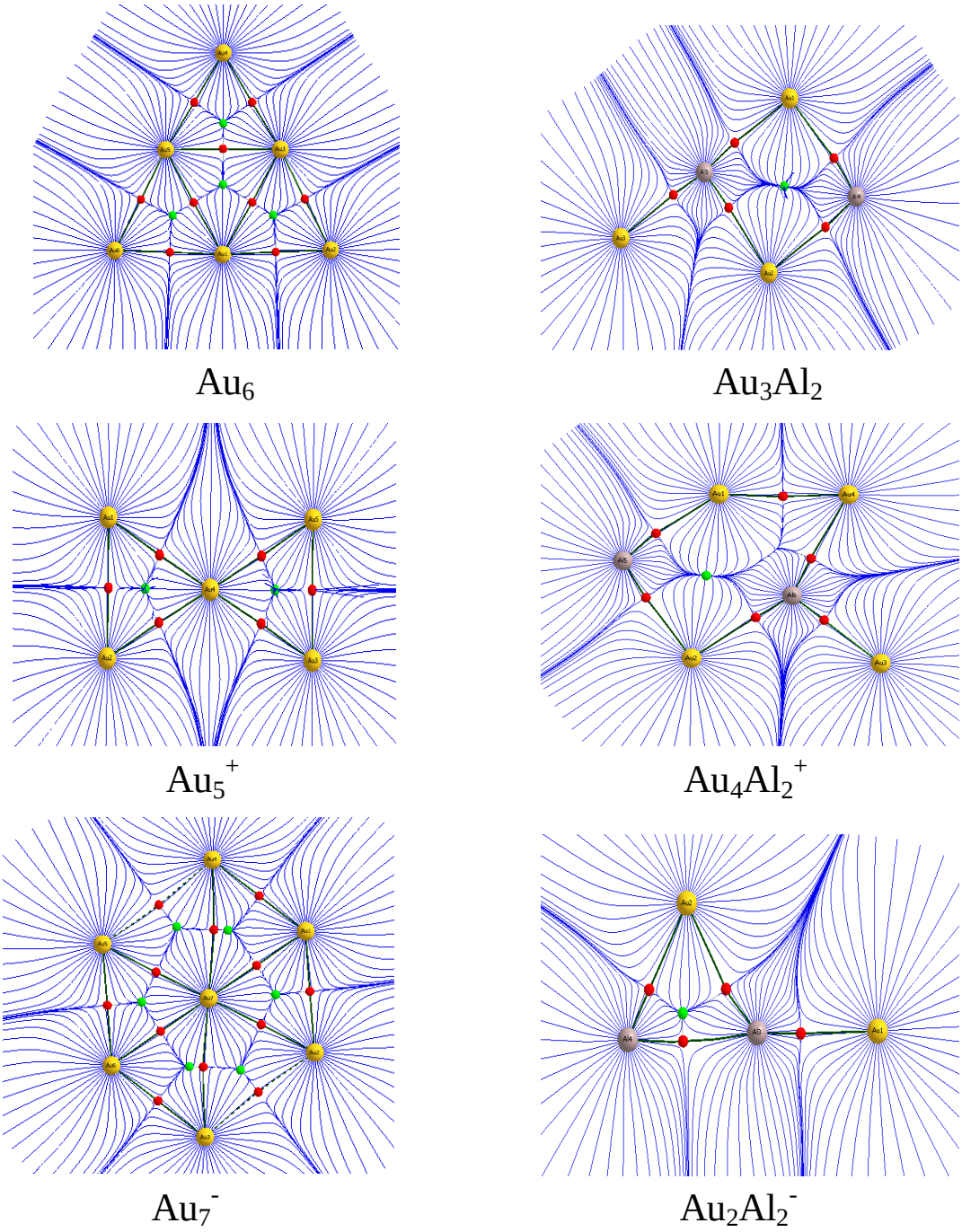

Figure 3.3.11 Trajectory field in some of the Au_n and Au_nAl_2 clusters. Gold and aluminium atoms are represented by yellow and grey spheres respectively. Bond paths and basin paths are indicated by dark green and blue lines, while the interatomic surfaces are indicated by dark blue lines. Red and green dots indicate bond critical points and ring critical points, respectively.

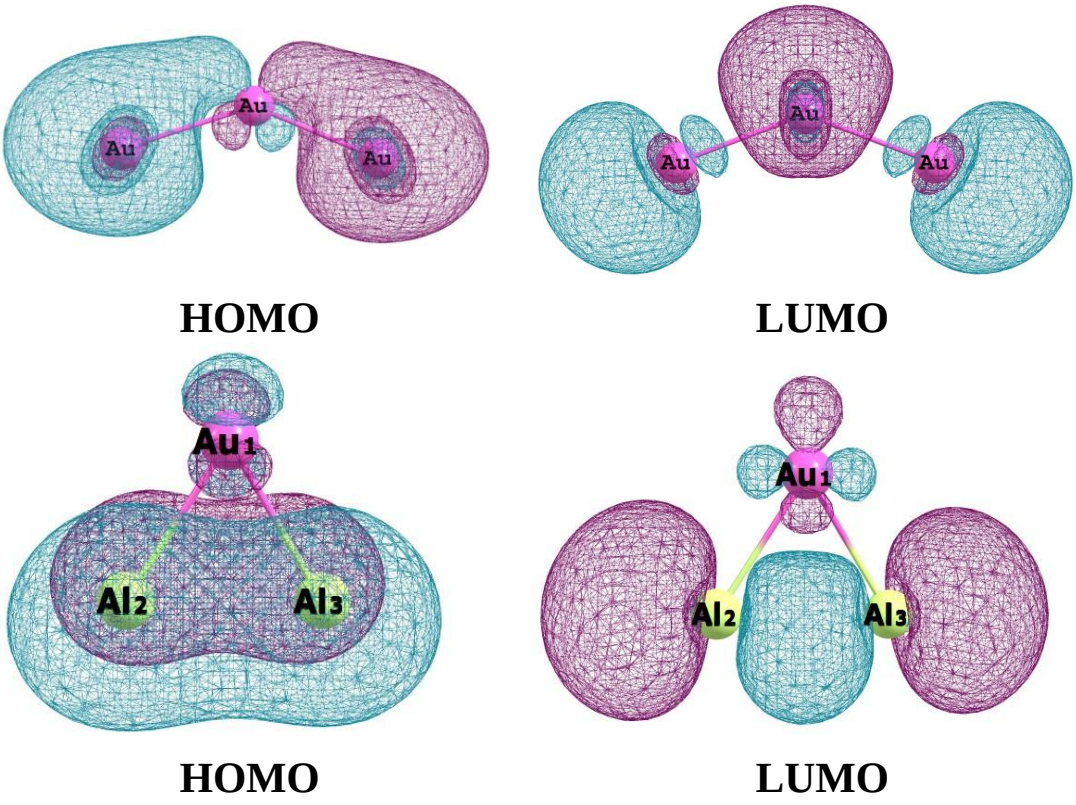

Figure 3.3.12 HOMO and LUMO isosurfaces of Au_3 and $AuAl_2$ clusters.

3.3.4 SALIENT OBSERVATIONS

A systematic study on the structures, stabilities and electronic properties of small bare gold Au_n and doubly Al doped Au_nAl_2 (neutral and charged) clusters using PW91PW91 level of theory is carried out here. The study provides us the following outcomes:

1. All the neutral Al doped Au_n clusters adopt plannar structures. This is in contrast to single Al doped clusters. The structures of doped clusters are different to that of pure clusters resluting the effect of doubly doped Al in the Au clusters. In the charged clusters a deviation is observed at n=3 and the doped clusters also have different geometries to that of pure clusters.
2. The study of relative stabilities results an even-odd oscillation. The binding energy plots clearly suggest the enhanced stability of the doepd clusters

compared to that of the pure ones. Among the doped clusters, Au_2Al_2, Au_4Al_2, , $Au_2Al_2^+$, $Au_3Al_2^-$ found to have greater stability in the region n=1-5.

3. The elctronic properties are expressed in terms of ionisation potential and electron affinity. The calculated values for the clusters show excellent agreement with the experimental results. Hence our studied structures are accurate. The lower values of VEA and higher values of VIP for the even numbered clusters indicate their higher stability compared to the odd ones.
4. The QTAIM study provies the presence of covant bond in the clusters. The electron density, ρ , and its Laplacian, $\nabla^2\rho$ at the Au–Au and Au–Al BCPs are found to be very small and positive.
5. Transfer of electron from Al to Au atoms is observed in natural charge analysis. This results the enhance stability of the doped clusters. The HOMO-LUMO isosurfacse further support the covalent behaiour of the clusters. Therefore, overall we can say that doping of two Al atoms can effectively increase the stability of the Au clusters.

BIBLIOGRAPHY

[1] Torres M.B., Ferna´ndez E.M. and Balba´s L.C. Theoretical study of oxygen adsorption on pure Au_{n+1}^+ and doped MAu_n^+ cationic gold clusters for M = Ti, Fe and n = 3–7. *Journal of Physical Chemistry A*, 112:6678–6689, 2008.

[2] Autschbach, J., Hess, B.A., Johansson, M.P., Neugebauer, J., Patzschke, M., Pyykko,¨ P., Reiher, M. and Sundholm, D. Properties of WAu_{12}. *Physical Chemistry Chemical Physics*, 6:11–22, 2004.

[3] Warner, J. Chemical aspects of the use of gold clusters in structural biology. *Journal of Structural Biology*, 127(2):106-112, 1999.

[4] Gaudry, M., Lermé, J., Cottancin, E., Pellarin, M., Vialle, J. L., Broyer, M., Prevel, B., Treilleux, M. and Mélinon, P. Optical properties of $(Au_xAg_{1-x})_n$ clusters embedded in alumina: evolution with size and stoichiometry. *Physical Review B*, 64(8):085407, 2001.

[5] Manzoor, D., Krishnamurty, S. and Pal, S. Effect of silicon doping on the reactivity and catalytic activity of gold clusters. *The Journal of Physical Chemistry C*, 118(14):7501-7507, 2014.

[6] Lopez, N. and Nørskov, J. K. Catalytic CO oxidation by a gold nanoparticle: a density functional study. *Journal of the American Chemical Society*, 124(38):11262-11263, 2002.

[7] Jakubke, H.-D. and Jeschkeit, H. Concise Encyclopedia Chemistry, Walter de Gruyter, Berlin, 1994.

[8] Balducci, G., Ciccioli, A. and Gigli, G. A mass spectrometric and density functional study of the intermetallic molecules AuBe, AuMg, and AuCa. *The Journal of Chemical Physics*, 121(16):7748-7755, 2004.

[9] Shao, P., Kuang, X. Y., Zhao, Y. R., Li, Y. F. and Wang, S. J. Equilibrium geometries, stabilities, and electronic properties of the cationic Au_nBe^+ (n= 1-8) clusters: comparison with pure gold clusters. *Journal of Molecular Modeling*, 18(8):3553-3562, 2012.

[10] Dong-Dong, C., Xiao-Yu, K., Ya-Ru, Z., Peng, S. and Yan-Fang, L. Geometries, stabilities, and electronic properties of Be-doped gold clusters: a density functional theory study. *Chinese Physics B*, 20(6):063601, 2011.

[11] Zhao, Y. R., Kuang, X. Y., Zheng, B. B., Wang, S. J. and Li, Y. F. Ab initio calculation of the geometries, stabilities, and electronic properties for the bimetallic Be_2Au_n(n= 1–9) clusters: comparison with pure gold clusters. *Journal of Molecular Modeling*, 18(1):275-283, 2012.

[12] Frisch, M.J., Trucks, G.W., Schlegel, H.B., Scuseria, G.E., Robb, M.A., Cheeseman, J.R., Scalmani, G., Barone, V., Mennucci, B., Petersson, G.A., Nakatsuji, H., Caricato, M., Li, X., Hratchian, H.P., Izmaylov, A.F., Bloino, J., Zheng, G., Sonnenberg, J.L., Hada, M., Ehara, M., Toyota, K., Fukuda, R., Hasegawa, J., Ishida, M., Nakajima, T., Honda, Y., Kitao, O., Nakai, H., Vreven, T., Montgomery, J.A., Jr., Peralta, J.E., Ogliaro, F., Bearpark, M., Heyd, J.J., Brothers, E., Kudin, K.N., Staroverov, V.N., Kobayashi, R., Normand, J., Raghavachari, K., Rendell, A., Burant, J.C., Iyengar, S.S., Tomasi, J., Cossi, M., Rega, N., Millam, J.M., Klene, M., Knox, J.E., Cross, J.B., Bakken, V., Adamo, C., Jaramillo, J., Gomperts, R., Stratmann, R.E., Yazyev, O., Austin, A.J., Cammi, R., Pomelli, C., Ochterski, J.W., Martin, R.L., Morokuma, K., Zakrzewski, V.G., Voth, G.A., Salvador, P., Dannenberg, J.J., Dapprich, S., Daniels, A.D., Farkas, Ö., Foresman, J.B., Ortiz, J.V., Cioslowski, J. and Fox, D.J. Gaussian 09, Revision A.1, Gaussian, Inc., Wallingford CT, 2009.

[13] Becke, A. D. Density-functional exchange-energy approximation with correct asymptotic behavior. *Physical Review A*, 38(6):3098, 1988.

[14] Lee, C., Wang, W., and Parr, R.G. Development of the Colle-Salvetti conelation energy formula into a functional of the electron density. *Physical Review B*, 37:785-789, 1988.

[15] Hay, P.J. and Wadt, W.R. Ab initio effective core potentials for molecular calculations. Potentials for the transition metal atoms Sc to Hg. *Journal of Chemical Physics*, 82:270-283, 1985.

[16] Hay, P.J. and Wadt, W.R. Ab initio effective core potentials for molecular calculations. Potentials for K to Au including the outermost core orbitals. *Journal of Chemical Physics*, 82:299-310, 1985.

[17] Barysz, M. and Pyykkö, P. Strong chemical bonds to gold. High level correlated relativistic results for diatomic $AuBe^+$, AuC^+, $AuMg^+$, and $AuSi^+$. *Chemical Physics Letters*, 285(5):398-403, 1998.

[18] Barrow, R. F., Gissane, W. J. M. and Travis, D. N. Rotational Analysis of the AX and BX Systems of AuBe and AuMg. *Proceedings of the Royal Society of London A: Mathematical, Physical and Engineering Sciences*, 287(1409):240-258, 1965.

[19] Bader, R. F. *Atoms in Molecules: A Quantum Theory*, Oxford University Press: Oxford, U.K. 1990

[20] Bader, R. F. A bond path: a universal indicator of bonded interactions. *The Journal of Physical Chemistry A*, 102(37):7314-7323, 1998.

[21] Bader, R. F. A quantum theory of molecular structure and its applications. *Chemical Reviews*, 91(5):893-928, 1991.

[22] AIMAll (Version 13.02.26), Todd A. Keith, TK Gristmill Software, Overland Park KS, USA, 2013 (aim.tkgristmill.com).

[23] Deka, A. and Deka, R. C. (2008). Structural and electronic properties of stable Aun (n= 2–13) clusters: a density functional study. *Journal of Molecular Structure: THEOCHEM*, 870(1):83-93, 2008.

[24] Zhao, Y. R., Kuang, X. Y., Zheng, B. B., Wang, S. J. and Li, Y. F. (2012). Ab initio calculation of the geometries, stabilities, and electronic properties for the bimetallic Be2Aun (n= 1–9) clusters: comparison with pure gold clusters. *Journal of Molecular Modeling*, 18(1):275-283, 2012.

[25] http://en.wikipedia.org/wiki/Magnesium

[26] Koyasu, K., Naono, Y., Akutsu, M., Mitsui, M. and Nakajima, A. Photoelectron spectroscopy of binary Au cluster anions with a doped metal atom: Au_nM^-(n= 2–7), M= Pd, Ni, Zn, Cu, and Mg. *Chemical Physics Letters*, 422(1):62-66, 2006.

[27] Majumder, C., Kandalam, A. K. and Jena, P. Structure and bonding of Au_5M (M= Na, Mg, Al, Si, P, and S) clusters. *Physical Review B*, 74(20):205437, 2006.

[28] Li, Y. F., Kuang, X. Y., Wang, S. J. and Zhao, Y. R. Geometries, stabilities, and electronic properties of small anion Mg-doped gold clusters: a density functional theory study. *The Journal of Physical Chemistry A*, 114(43):11691-11698, 2010.

[29] Plus, F. Accelrys Inc., San Diego, CA, 2008.

[30] Rappé, A. K., Casewit, C. J., Colwell, K. S., Goddard Iii, W. A. and Skiff, W. M. UFF, a full periodic table force field for molecular mechanics and molecular dynamics simulations. *Journal of the American Chemical Society*, 114(25):10024-10035, 1992.

[31] Antonello, S., Arrigoni, G., Dainese, T., De Nardi, M., Parisio, G., Perotti, L., René, A., Venzo, A. and Maran, F. Electron transfer through 3D monolayers on Au_{25} clusters. *ACS Nano*, 8(3):2788-2795, 2014.

[32] Huber, S. E., Warakulwit, C., Limtrakul, J., Tsukuda, T. and Probst, M. Thermal stabilization of thin gold nanowires by surfactant-coating: a molecular dynamics study. *Nanoscale*, 4(2):585-590, 2012.

[33] Perdew, J. P., Chevary, J. A., Vosko, S. H., Jackson, K. A., Pederson, M. R., Singh, D. J. and Fiolhais, C. Atoms, molecules, solids, and surfaces: Applications of the generalized gradient approximation for exchange and correlation. *Physical Review B*, 46(11):6671, 1992.

[34] Häkkinen, H., Yoon, B., Landman, U., Li, X., Zhai, H. J. and Wang, L. S. On the electronic and atomic structures of small Au_n^-(n= 4− 14) clusters: a photoelectron spectroscopy and density-functional study. *The Journal of Physical Chemistry A*, 107(32):6168-6175, 2003.

[35] Cheeseman, M. A. and Eyler, J. R. Ionization potentials and reactivity of coinage metal clusters. *The Journal of Physical Chemistry*, 96(3):1082-1087, 1992.

[36] Bouwen, W., Vanhoutte, F., Despa, F., Bouckaert, S., Neukermans, S., Kuhn, L. T., Weidele, H., Lievens, P. and Silverans, R. E. Stability effects of

$Au_nX_m^+$(X= Cu, Al, Y, In) clusters. *Chemical Physics Letters*, 314(3):227-233, 1999.

[37] Wang, C. J., Kuang, X. Y., Wang, H. Q., Li, H. F., Gu, J. B. and Liu, J. Density-functional investigation of the geometries, stabilities, electronic, and magnetic properties of gold cluster anions doped with aluminum: Au_nAl^- ($1 \leqslant n \leqslant 8$). *Computational and Theoretical Chemistry*, 1002:31-36, 2012.

[38] Zhao, L.X., Feng, X.J., Cao, T.T., Liang, X. and Luo, Y.H. Density functional study of Al doped Au clusters. *Chinese Physics B*, 18(7):2709-2718, 2009.

[39] Li, Y. F., Mao, A. J., Li, Y., and Kuang, X. Y. (2012). Density functional study on size-dependent structures, stabilities, electronic and magnetic properties of Au_nM (M= Al and Si, n= 1–9) clusters: comparison with pure gold clusters. *Journal of Molecular Modeling*, 18(7):3061-3072, 2012.